Surveys in Geophysics (2005) 26:733–765
DOI 10.1007/s10712-005-1832-1

ANISOTROPY VERSUS HETEROGENEITY IN CONTINENTAL SOLID EARTH ELECTROMAGNETIC STUDIES: FUNDAMENTAL RESPONSE CHARACTERISTICS AND IMPLICATIONS FOR PHYSICOCHEMICAL STATE

PHILIP E. WANNAMAKER
Energy & Geoscience Institute, University of Utah, 423 Wakara Way, Suite 300, Salt Lake City, UT, 84108, U.S.A
E-mail: pewanna@egi.utah.edu

(Received 14 January 2005; accepted 25 May 2005)

Abstract. Electrical anisotropy, the effect of current density in a medium being a function of the orientation of the electric field, is being recognized increasingly as an important effect in explaining Earth electromagnetic observations. A consideration of anisotropy, however, in most cases is an admission of spatial aliasing in earth structure, wherein the averaging volume of diffusive EM fields may be greater than the characteristic dimensions of a family of oriented structures, thus leading to a response which is equivalent to a bulk anisotropic medium. Even for two-dimensional geometries, there can be strong non-parallelism of principal axes of vertical magnetic field relative to the impedance over broad areas, as well as impedance phase variations which leave normal quadrants, if there are multiple directions of anisotropy or anisotropy strike distinct from bulk geometric (2D) strike. This paper concentrates on experience with regional field studies in continental settings where bulk anisotropy is apparent. Upper crustal anisotropy may result from preferred orientations of fracture porosity, or lithologic layering, or oriented heterogeneity. Lower crustal anisotropy may result from preferred orientations of fluidized/melt-bearing or graphitized shear zones, but does not necessarily reflect current state of stress *per se*. In the upper mantle, the prior causes all may act in pertinent domains, but added to these is the possibility of strong electrical anisotropy due to hydrous defects within shear-aligned olivine crystals (solid-state conduction). Several field examples from continental MT investigations will be discussed, which roughly fall into active transpressional, active transtensional, and fossil transpressional regimes. A general challenge in interpreting data with apparent anisotropic effects is to establish the tradeoff between heterogeneity and anisotropy in the inversion of EM responses.

Keywords: Electromagnetics, anisotropy, magnetotellurics, solid-earth

1. Introduction

With electrical anisotropy, current density depends on the direction of the electric (E) field, and the direction of current is not necessarily parallel to the E-field direction (e.g., Edwards et al., 1984; Weidelt, 1999; Wang and Fang,

2001). Understanding this property has large implications for economic resource evaluation, interpretation of hydrological flows, and models of material composition and transport in the deep crust and upper mantle. To a large extent, consideration of anisotropy reflects the inability to resolve oriented heterogeneity below a certain spatial limit. Given that the resolving power of diffusive EM methods like magnetotellurics (MT) diminishes with depth to target, the spatial limit below which only equivalent anisotropy is resolvable becomes increasingly broad with depth. Elucidation of mixing laws for multicomponent media to determine bulk electrical properties has been a constant challenge.

In this paper, I consider mainly experience with electrical anisotropy apparent in MT data from regional electromagnetic surveys, particularly for the plane-wave source of MT. After a brief introduction to the property, an overview of the state of modeling of MT responses over anisotropic media is presented. A few fundamental characteristics of such responses are highlighted. Subsequently, the bulk of the presentation pertains to observed apparent anisotropic responses and their implications for physical state of the deep crust and upper mantle in various continental tectonic regimes. Oceanic conductivity and its anisotropy are addressed in the companion review paper by Baba (2005). The paper closes with a list of challenges remaining in the interpretation of anisotropy in multidimensional environments.

2. Basic Characteristics of Anisotropy

In anisotropic problems, the conductivity is considered to be a tensor (e.g., Weidelt, 1999, and many others). Generally, it is of rank 3 but symmetric for purely ohmic conduction, and non-negative definite (Figure 1). With the exception of microscopic intracrystalline anisotropy which we will consider later, bulk anisotropy at the resolving scales of diffusive EM measurements is typically the result of mixing in a preferred orientation of two or more media types of differing conductivities. A very simple view of this appears in Figure 1 with adjacent media of two differing conductivities being subject to an oblique applied electric field. For this laminar geometry, the average current density over both objects is canted toward the 'strike' direction relative to the average electric field. However, for a non-negative conductivity tensor, the angle between average electric field and current density remains acute (Weidelt, 1999).

For a simple laminar geometry, the bulk resistivities normal (n) and parallel (p) to the laminae are (e.g., Heise and Pous, 2001; Wang and Fang, 2001):

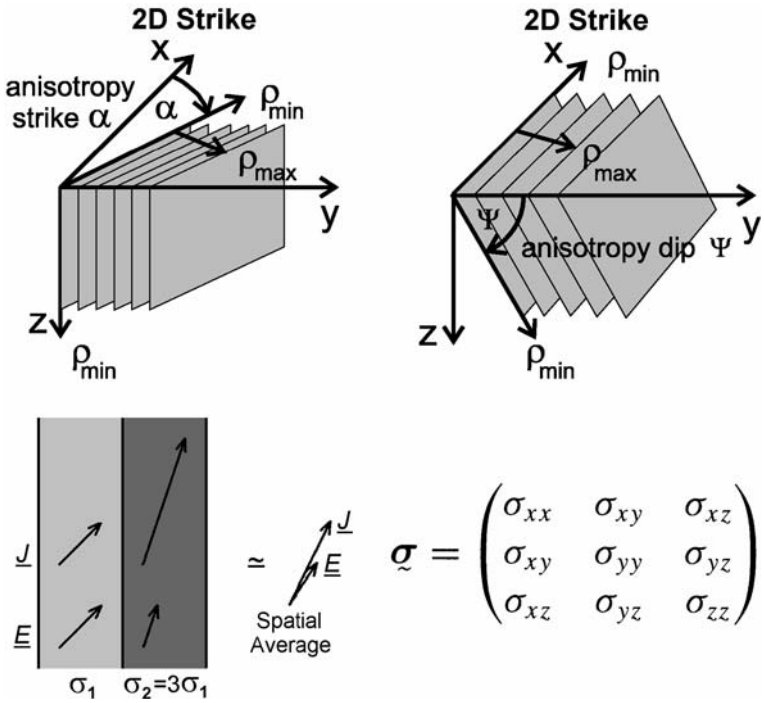

Figure 1. Example representations of anisotropy in earth materials. Anisotropy often is represented in terms of minute alternating planes of different conductivity with strike (sometimes also called azimuth) and dip which may be non-parallel to geometric strike. In anisotropic media, electric field and current vectors are not necessarily parallel. Figures from Heise and Pous (2001) and Weidelt (1999), with permissions from the authors.

$$R_n = (1 - V_1)R_2 + V_1 R_2 \tag{1a}$$

and

$$1/R_p = (1 - V_1)/R_2 + V_1/R_2 \tag{1b}$$

where V_1 is the volume fraction of material 1. Analogous relations in terms of dike widths are given by Eisel and Haak (1999) and similar relations can be derived for infinite orthogonal thin rod-like geometries. Weidelt (1999) derives semi-quantitative bounds on anisotropy for two-dimensional (2D) media with two embedded phases using a homogenization theory.

Real-world bulk anisotropies more often may reflect oriented conducting elements, which are imperfectly connected over larger scales. An interesting approach to quantifying this situation has been pursued using embedded fractal random resistor networks (Bahr, 1997, 2000; Bahr et al., 2002) (Figure 2). To a large degree, it proceeds from analogous study of fluid flow

in fractal networks by Gueguen et al. (1991). The analysis points out that the highest degrees of bulk anisotropy may result from slight changes in connection of the higher-conducting phase if it remains close to its percolation threshold. This in fact represents a situation where most of the conducting phases have a rather low degree of long-range electrical connectivity. The range of possible anisotropy tends to increase with the order of fractal embedding. In the field MT and geological studies reviewed, conducting elements in nature are argued to be disposed under petrological and structural/rheological controls. The fractal model example just described can then be compared to other scenarios of establishing preferred directions of conduction.

3. State of Numerical Simulation of Anisotropic MT Responses

Excellent discussions of the history and state of anisotropic modeling for plane wave and finite sources over 1D earth models has been given by Josef

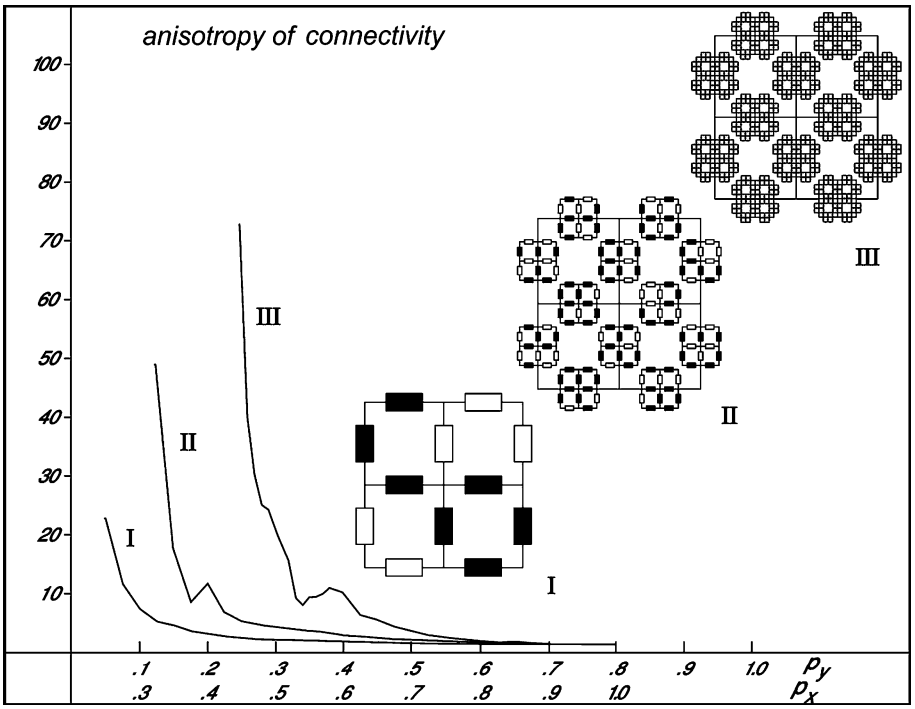

Figure 2. Anisotropy of electrical conductivity found by numerical random resistor experiments for simple network (I), embedded network (II), and twice-embedded network (III). The probabilities p_x and p_y that bonds oriented in the two perpendicular directions x and y are not blocked differ by only 20%. In region III, each lowest-level cluster is assumed to have random distribution similar to I. Redrawn from Bahr (1997), with permission of the author.

Pek and coworkers (Pek and Santos, 2002; Pek, 2002; Kovacikova and Pek, 2002a, b). Pek and Santos (2002) show that the governing equations for the horizontal electric fields in each layer of the 1D earth can be expressed in terms of reduced aggregate conductivities A_{ij}, according to:

$$\frac{\partial^2 E_x}{\partial z^2} + \mathrm{i}\omega\mu_0(A_{xx}E_x + A_{xy}E_y) = 0, \tag{2a}$$

$$\frac{\partial^2 E_y}{\partial z^2} + \mathrm{i}\omega\mu_0(A_{yx}E_x + A_{yy}E_y) = 0, \tag{2b}$$

where

$$A_{xx} = \sigma_{xx} - \frac{\sigma_{xz}\sigma_{zx}}{\sigma_{zz}}, \quad A_{xy} = \sigma_{xy} - \frac{\sigma_{xz}\sigma_{zy}}{\sigma_{zz}}, \tag{3a}$$

$$A_{yx} = \sigma_{yx} - \frac{\sigma_{yz}\sigma_{zx}}{\sigma_{zz}}, \quad A_{yy} = \sigma_{yy} - \frac{\sigma_{yz}\sigma_{zy}}{\sigma_{zz}} \tag{3b}$$

and $A_{xy} = A_{yx}$ from symmetry. Thus, plane–wave EM field responses do not allow reconstruction of the full conductivity tensor of a layer (or even a half-space), and in principle an unlimited number of tensors could possess the same aggregate conductivities. The 1D MT problem for a generally anisotropic layered medium can always be set up as an equivalent azimuthally anisotropic structure incorporating the elements of the rank-3 layer tensors. Finite source fields in principle have some sensitivity to anisotropy dip, but this was judged to be weak for realistic anisotropy contrasts (Pek, 2002).

Perhaps the best-known algorithm for MT responses over 2D structures with generally oriented anisotropy is that of Pek and Verner (1997), building on the work of Reddy and Rankin (1975). One motivation for this development was the observation in field data (to which we will return later) that sometimes there is a systematic discrepancy between the MT impedance principal directions and those implied by the vertical magnetic field (H_z) induction arrows. The algorithm has been extended to include topography and bathymetry by Pek and Toh (2001). An extension of the Rodi and Mackie (2001) 2D MT inversion program to include a diagonalized conductivity tensor has been created for application to seafloor MT data (Baba et al., 2005). This approach yields separate images for along-strike, cross-strike, and vertical resistivity components. It achieves stability by damping the departures of the three principal resistivities from each other. However, it does assume that the axes of anisotropy are known, i.e., coincide with the Cartesian axes of the 2D model framework. Inversion for 2D structure with more arbitrary anisotropy orientations was presented by Li et al. (2004).

The Pek and Verner 2D algorithm was used by Heise and Pous (2001) to test the effect of anisotropy strike orientations on equivalent isotropic 2D inversions. The example of Figure 3 considers two levels of isotropic media over an anisotropic basal half-space having a 20:1000 resistivity contrast, with variable anisotropy strikes tested. Impedance principal axes determined the imposed anisotropy strike angle, and joint TE–TM mode inversions with strike defined at the anisotropy angle recovered much of the true structure. Below a depth of about 20 km in the inversion model, the anisotropy of the basal medium is represented by alternating conductive and resistive dike-like media, whose integrated lateral average conductivities (across and along strike) reproduce those of the anisotropic medium reasonably well. An alternative type of inversion in this author's view is to initially perform a single mode inversion (e.g., TM only), or possibly combine modes for the period range where uniform strike angle is apparent. A subsequent inversion of the other mode's data, subject to keeping the conductivity variations close to the initial inversion, could yield a smoother estimate of the deep anisotropic conductivities.

The effect of anisotropy in the basement upon the induction arrow direction at various periods, and the effect of anisotropy strike on arrow direction at a fixed period, was also studied by Heise and Pous (2001) (Figure 4). The induction arrows tend to be deflected from being normal to the overlying 2D isotropic structure, towards the anisotropy strike. Currents perpendicular to the strike of the overlying isotropic structures, induced by the magnetic field parallel to strike, are deflected in the direction of preferred current flow in the anisotropic medium below, thus rotating the induction arrows (Pek and Verner, 1997). Dramatic effects upon impedance phase behavior also are possible when anisotropy strikes of upper and lower structures differ greatly and are substantially non-parallel to the geometric strikes of the 2D bodies (Pek and Verner, 1997). In particular, phase values

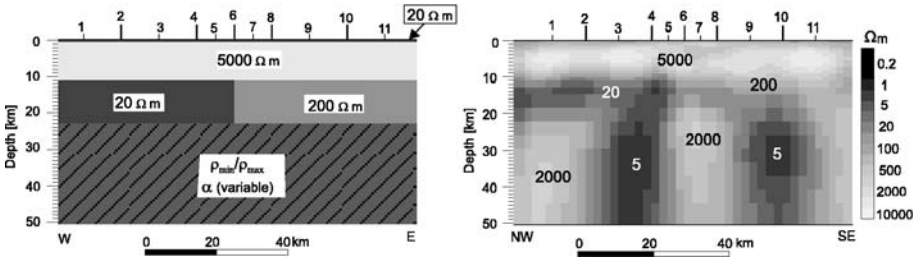

Figure 3. Left: 2D model with contacting isotropic slab having a 1:100 resistivity contrast beneath resistive overlying layer, placed on anisotropic basement with anisotropy strike not necessarily parallel to geometric strike. Right: isotropic 2D inversion model for data rotated clockwise 30° to the anisotropy strike of this particular model. The 20:1000 anisotropy factor in the basement is replicated by alternating conductive and resistive dike-like media. Replotted from Heise and Pous (2001).

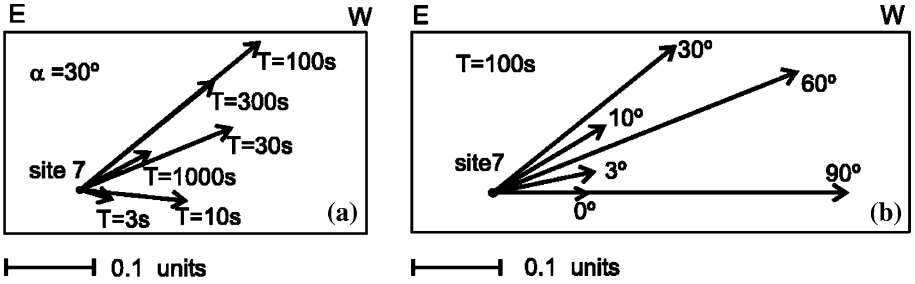

Figure 4. Orientation of induction arrows for 2D model of Figure 3 and an anisotropy strike of 30° at various periods (a) and various anisotropy strikes at $T = 100$ s (b). Replotted from Heise and Pous (2001).

out of their natural quadrants can occur where locally the projection of the electric field along a particular cartesian component becomes reversed from the direction of the component current density. This was verified and explored further by Heise and Pous (2003), who noted that the effect was limited to the domain of the shallower, smaller scale structure and that the regional structure could be recovered. Pek and Verner stress, however, that the total vector current density and electric field cannot be anti-parallel due to the non-negativity of the conductivity tensor in the Earth.

For the fully 3D anisotropic problem, several forward problems have emerged involving either plane wave or EM finite sources (Weidelt, 1999; Davydycheva and Drushkin, 1999; Wang and Fang, 2001; Weiss and Newman, 2002). Deflection of induction vectors away from symmetry axes by anisotropic current flow is confirmed in model studies by Weidelt, who also emphasized that anisotropic models cannot explain responses that are not interpretable by isotropic 3D models of arbitrary complexity. To quote, 'all anisotropy can be explained by structural anisotropy resulting from spatial averages over isotropic structures with a preferred orientation'. To this author's knowledge, no explicit 3D inversion algorithm including both anisotropy and heterogeneity has yet emerged. Challenges can be anticipated in jointly solving for optimal values of anisotropic conductivity and anisotropy orientations, unless the latter can confidently be assumed. With incorrectly assumed orientations, equivalent alternating elongate structures analogous to those of Figure 3 in the 2D case (lumped isotropic structures) seem likely to arise to some extent.

4. Field Surveys Exhibiting Apparent Anisotropy, and Physical Implications

Sufficient experience with field data has built up for the community to realize that it is very common for the interpreted conductivity in one horizontal

direction to differ significantly from that of the orthogonal direction, even for situations that seem well approximated by 2D geometries. A fortunate aspect of straightforward 2D anisotropy is the greater confidence one may have with 2D isotropic inversions if properly constructed and interpreted. Hence, we may be on firmer ground in making tectonic or petrological inferences from those conductivity models. As introduced, however, a consistent obliquity between impedance principal axes and strike based on vertical magnetic field, extremes in response behavior often with high local variability, and rotations of principal directions at longer periods from apparent geological trends at the surface, have been seen in several field surveys and have motivated modeling developments (e.g., Pek and Verner, 1997).

In this section, I summarize several MT transect interpretations on the continents which exemplify apparent bulk anisotropic behavior in certain instances and discuss what they suggest about conductivity mechanisms. These areas cover regimes of active transpression, active transtension, and fossil transpression. The laboratory-based understanding of anisotropy controls is worked in during the discussion of causes of the anisotropy in the field models. Laboratory here is taken to include not only small-scale P–T experiments or calculations with Earth materials per se, but also large scale inferences on geochemical or structural state from field geological studies. The review is by no means exhaustive, but is meant to represent at least some important orogenic processes which manifest well-developed anisotropic conductivity structures.

4.1 Active Transpressional Regimes

As one example of this regime, the New Zealand Southern Alps is a highly oblique compressional regime exhibiting high rates of mountain uplift and a well-developed crustal root zone (Wannamaker et al., 2002). A low resistivity zone in the lower crust developed in and over the crustal root is interpreted to reflect fluids generated through prograde metamorphism, and interconnected in ductile shear zones (lower crust) and stockwork fracture zones (upper crust) (Figure 5). The structure is accompanied by a seismic low-velocity anomaly. Impedance decomposition indicated a strike direction of N40°E, or $\sim$15° ccw from the strike of the Alpine Fault, over the period range most affected by the deep conductor, a deviation which is resolvable but otherwise not considered troublesome. The nominal TE mode impedance and H_z-field data imply significantly greater conductivity in the lower crust along electrical strike than across it. The TE image shown in Figure 5 was derived by keeping the model as close as possible to the TM image, and thus exhibits a relatively simple lateral character. Joint TE–TM inversion yields a model much 'clumpier' in texture (Wannamaker et al., 2002, not shown

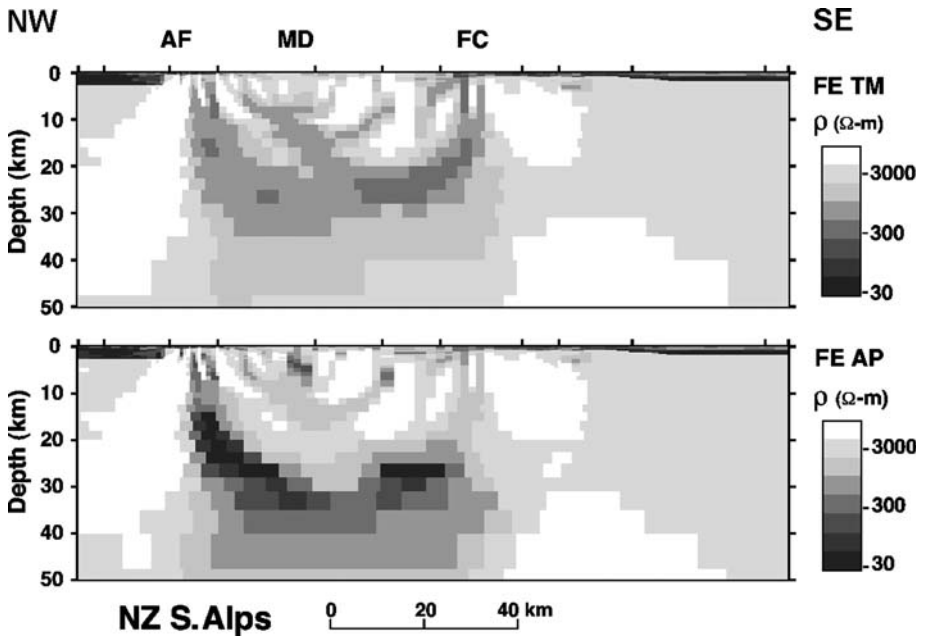

Figure 5. Coast-to-coast, 2D resistivity cross sections from inversion of TM mode (cross-strike) impedance data (top) and of TM + H_z data (bottom) (replotted from Wannamaker et al., 2002). Physiographic features include Alpine Fault (AF), Main Divide (MD), and Forest Creek fault zone (FC). Section runs northwest (NW) to southeast (SE). Granularity of model with increasing depth reflects growth in regularization parameters.

here), similar to the joint images of Heise and Pous (2001), which preserves significant current flow along strike but restricts current flow across strike in order to fit the two modes at once.

Electrical anisotropy is not unexpected in transpressional regimes due to formation of shear zones with preferred orientation. Shear zone elements fall into three categories: isolated, dangling, and backbone (Cox et al., 2001) (Figure 6). Over time, fault zones initiate across a broad span of anastomozing faults, with narrower, through-going faults becoming the product of increased strike-slip displacement (e.g., Sibson, 2000). In other words, the degree of long-range fluid interconnection represented by the throughgoing backbone structures increases with degree of shearing. Note that just above the percolation threshold of backbone formation, the long-range backbone structures constitute only a small fraction of the total fault population which can access fluids. However, the percolation threshold for backbone elements is interpreted to be reached for 3D fault arrays at bulk strains of only a few percent (Cox et al., 2001). Thus, in terms of the previously introduced percolation theory of Figure 2, substantial anisotropy could occur in the early stages of transpression. Degree of anisotropy could increase with progressive

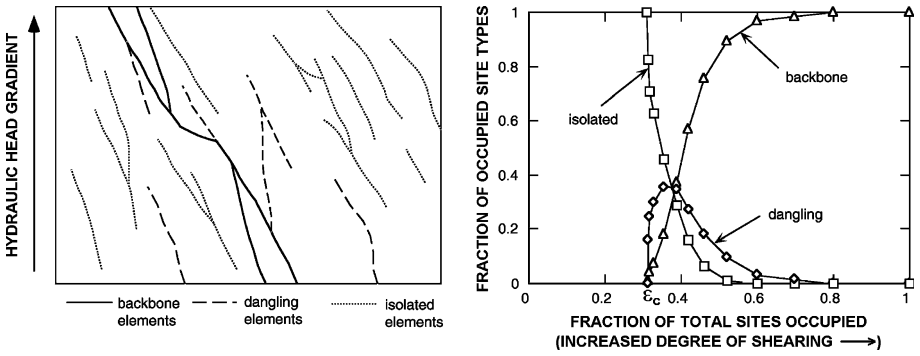

Figure 6. (a) Schematic 2D depiction of a fault network consisting of isolated elements, dangling elements, and backbone elements. Most flow occurs in the backbone, while fluid is fed to and discharged from the backbone via dangling elements. (b) Fraction of total fault element population occupied by each element type subsequent to strain reaching a critical degree ε_c (percolation threshold). At this degree, essentially all faults are isolated, but dangling and backbone elements begin to form. At very high strain degrees, the great majority of faults have become throughgoing backbone elements. Modified from graphic provided by S. Cox.

shearing because degree of interconnection along strike should increase, and there may be a tendency for shears to further 'self-organize' into backbone elements through fluid-driven weakening and growth (Cox et al., 2001). Alternately, conduction may be limited if fluid flow is episodic and spatially limited along the backbones.

MT profiling in the southern Chilean Andes described by Brasse and Soyer (2001) detected strong conductive anomalies in the lower crust under the volcanic arc, correlated with high-temperature fluids and melting. Impedance principal directions were nearly N–S for the profiling, close to paralleling the volcanic chain and the subduction trench, motivating a 2D interpretation. However, further analysis revealed that the magnetic induction (H_z) strikes in the survey showed a consistent tilt nearly 45° East of North (Figure 7). A forward model incorporating anisotropy in the lower crust reproduces this feature reasonably well, requiring an anisotropy strike of 45° and along-strike conductivities several times greater than those across strike (Li, Brasse, and Soyer, unpublished data). Nevertheless, the basic features of lower crustal conductivity structure remain in accord with the original 2D inversion of Brasse and Soyer, similar to the experience of Heise and Pous (2001). Pre-subduction fault trends in the area are observed which also trend to the northeast (H. Brasse, personal communication), suggesting that ancestral structures exert an important control on present conductivity. However, an interesting implication of this is that the new N–S tectonic grain did not make significant use of pre-existing structural orientations for its tectonic development.

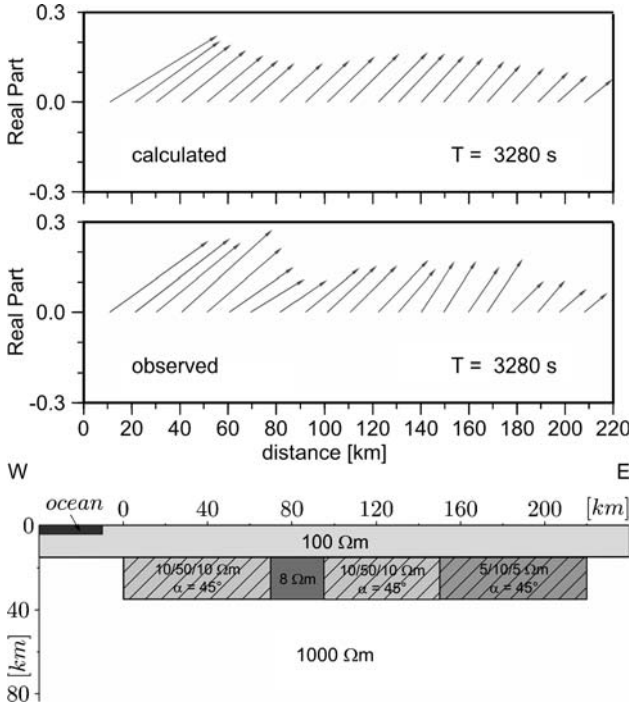

Figure 7. Observed and computed magnetic induction strikes for profile of MT stations across the southern Chilean Andes and the corresponding 2D anisotropic model (H. Brasse, pers. comm.). Resistivity values in the model correspond to along-strike, across-strike, and vertical directions respectively. Results computed with program developed by Y. Li.

4.2 Active Transtension

Dense MT profiling was carried out in the active extensional Great Basin province of north-central Nevada, western United States, by Wannamaker and Doerner (2002) in a study of metamorphic core complex development and thermal processes. It is a complex area experiencing Phanerozoic continental margin sedimentation, two major compressional orogenies, two extensive plutonic suites, and two major episodes of extension. While current surface Basin–Range morphology trends are NNE, the initial direction of extension was NNW, possibly influenced by ancestral trends of the early Paleozoic continental margin (Zoback et al., 1994). The earlier direction exerted control on world-class Carlin-trend gold deposits and on the earliest basaltic magmatism (Wannamaker and Doerner, 2002).

Decomposed impedance strike estimates based on the method of Bahr (1988) for long periods ($20 < T < 1000$ s) showed that lower crustal electrical strike lay ~N20°W (Sodergren, 2002), similar to the pre-Basin and Range structures. Tipper element values were small (< 0.1) in this period range. To assess bulk lower crustal anisotropy at the broadest scales, the

off-diagonal impedance elements in the $x = \text{N20°W}$ coordinate frame were integrated over the profiling to obtain a single average tensor sounding (Figure 8). For the nominal TM(yx) mode at least, this is approximately equivalent to laying a single measurement bipole over the entire profile (~80 km), and suppresses the effects of lateral heterogeneity (Torres-Verdin and Bostick, 1992). Intriguingly, both the TE and the TM apparent resistivities and phases approach common values for periods shorter than about 3 s (Figure 8), and they are similarly common values as seen for other profiling in the eastern Great Basin described by Wannamaker et al., (1997). Thus, despite the extensive tectonism producing a visible NNE grain to the morphology today, no longer-wavelength anisotropy in the upper crust has developed. Bulk apparent resistivities for $T < 10$ s appear to reflect mainly the original Paleozoic margin sedimentary section dominating the lithologies of the central and eastern Great Basin. That the TE graben responses also have effectively been averaged out is interpreted to reflect that, in this case, substantial bodies of alluvium lie off-profile as well as along it. Of course, individual soundings can show marked apparent anisotropy due to individual horst-graben structures, as seen also in the study of Adam (1996) of the extensional Pannonian Basin.

However, for a NNW orientation of the x-axis, the nominal TE(xy) data imply that bulk resistivities of the lower crust in the area are 3–4 times lower than for the TM mode. A view of the lower crustal anisotropy for current flow in the NNW and ENE directions is given in Figure 9, derived from

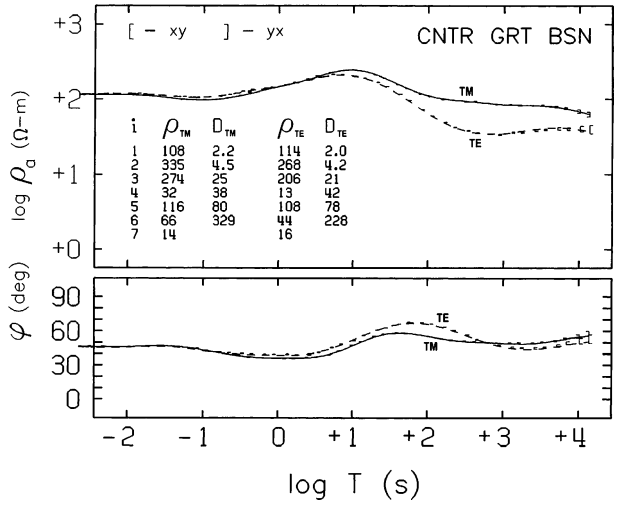

Figure 8. Integrated impedance soundings for MT data rotated to N20W with fit of smooth 1D inversion. Both TE and TM mode data are shown. Error bars are smaller than the plotting symbols. Layered earth inversion also was performed, and layering parameters (R = resistivity in Ωm, D = depth in km) are tabulated in the figure. Modified from Sodergren (2002).

smoothed and layered 1D inversion (Sodergren, 2002). Lower crustal conductance in the NNW direction is 3–4 times greater than for the ENE direction.

The cause of the lower crustal conductor in the Great Basin is believed to be hypersaline fluids and water-undersaturated partial melts, because volcanic products imply that oxygen fugacity is too high to support graphite (Wannamaker et al., 1997; 2001). Hence, the question arises as to whether the anisotropy is the result of the present day stress regime, or of existing fabric in the rock controlling fluid distribution. Current strain directions are directly E–W or perhaps even ESE–WNW, consistent with horst-graben directions, based on precise geodetic surveying (Hammond and Thatcher, 2004) which does not support current stress as the cause. Moreover, in feldspathic lithologies, stress is shown to improve the degree of fluid interconnection but the connection is not anisotropic (Tullis et al., 1996). Thus, existing fabric in the high-grade Proterozoic metaigneous basement to the region is favored as the cause of the anisotropy through controls on the orientation of the fluid or melt. A picture of how this exists may be that of Sawyer (2001), based on field interpretations in migmatitic terranes (Figure 10). Sites of formation or resorption of partial melt are concentrated along foliations of hydrous minerals which are essential components of melt reactions, and we presume that disposition of saline fluids at somewhat lower

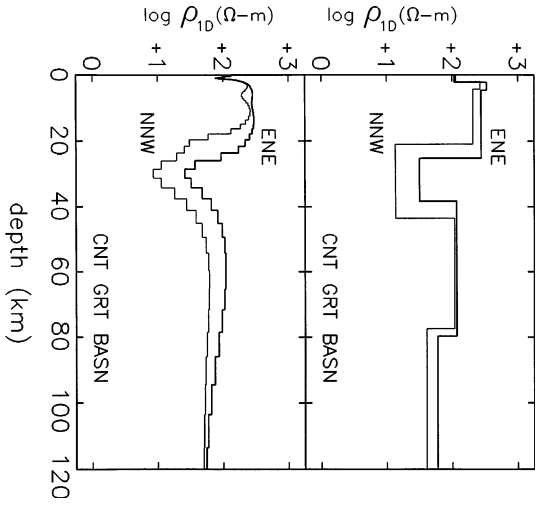

Figure 9. Smooth (left) and layered (right) 1D inversion models of the TE (NNW) and TM (ENE) integrated impedance responses of Figure 8. The smooth inversion is an *a priori* adherence algorithm written by the author follow Tarantola (1987), using a 100 Ωm half-space as the reference model. Sensitivity tests in Sodergren (2002) for the layered inversion showed that the bottom of the conductive layer for both modes can reside at a common depth of ~39 km (near Moho) and still fit the data.

temperatures involving hydrate reactions can occur similarly. Hence, ancient fabric controls modern fluid orientation and resistivity anisotropy. That the bottoms of such conductive layers lie near the Moho may reflect the greater ease of fluid interconnection in crustal mineralogies relative to those of the upper mantle (e.g., Watson and Brenan, 1988).

Western and central Europe is under a moderate state of extensional stress as evident from existence of the Rhine graben and Tertiary volcanism (Blundell et al., 1992). Crustal and upper mantle scale resistivity structures of the region have been modeled and described by Bahr and Duba (2000), Leibecker et al. (2002), and Gatzemeier and Moorkamp (2005). Leibecker's 3D forward model for the crust is shown in the upper part of Figure 11. A conductive (0.5 Ωm) body in the upper crust was interpreted as hot, hypersaline fluids, although it is tempting with such low values to consider a cryptic graphitic body. Anisotropy in the middle crust is oriented in a broadly NE–SW direction, and is correlated with graphitic conducting elements in fossil trends of the Hercynian orogenic belt of north central Europe. No clear evidence of the current N–S oriented Rhine graben structures occurs in the data.

In the upper mantle in the 100–150 km depth range, long period impedance phase splits over the region imply that the resistivity at such depths is highly anisotropic. Bulk resistivity in the E–W direction is 1–2 Ωm while that in the N–S is ~250Ω m (Gatzemeier and Moorkamp, 2005). The resistivity in the more conductive direction would require ~10% of aligned melt, the mechanical stability of which is questionable. Gatzemeier and Moorkamp

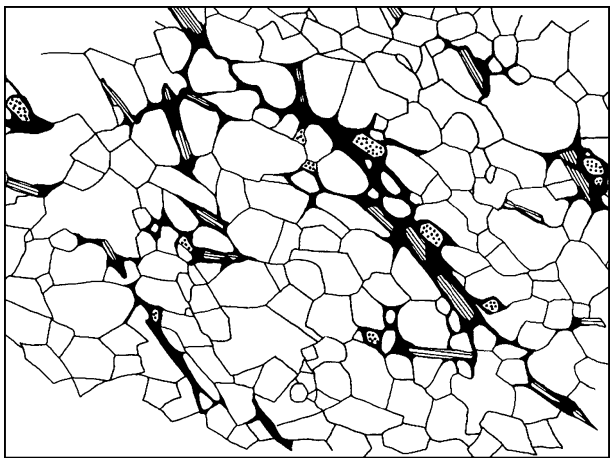

Figure 10. Schematic development of melt pools along foliation planes, based on outcrop mapping in migmatitic terranes (Sawyer, 2001, reproduced with permission). Foliation is defined by biotite (striped pattern) in a matrix of quartz and feldspar (white). Melt is black and dotted minerals are melt-produced pyroxene.

(2005), based on an expanded array compared to the earlier work of Leibecker et al. (2002), argue that the E–W resistivity is non-uniform areally, being the lower to the North, and also is terminated to the East and South. These authors, and Bahr and Duba (2000), suggested that the highly directional conductivity may be due to aligned olivine crystals which contain a significant volume of hydrous defects in the solid state. This follows the initial suggestion of Karato (1990).

An idealized illustration of the possible influence of hydrous defects appears in Figure 12 following Karato (1990) and Lizzaralde et al. (1995), but using newer estimates of solubility and anisotropic defect diffusivities (Kohlstedt and Mackwell, 1998; Simpson, 2002; Bell et al., 2003; Zhao et al., 2004; Simpson and Tommasi, 2005). In the plot are hypothetical resistivity profiles for two geotherms: a high-temperature regime (90 mWm^{-2}) such as the northern Basin and Range (BR), and a stable geotherm (45 mWm^{-2}) (ST) (Lachenbruch et al., 1978). The stable geotherm follows the global average current mantle adiabat (ACMA) (Thompson, 1992) below ~180 km depth.

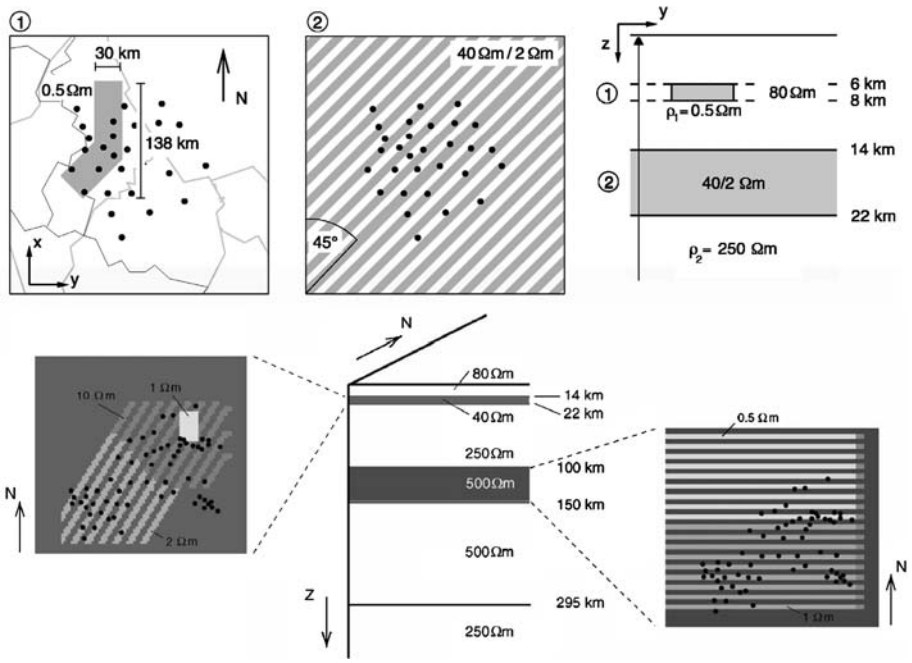

Figure 11. A 3D model of the resistivity below the Rhenish shield area. Upper left and middle: Plan view of two inhomogeneous layers at 6 and 14 km depth. Upper right: Vertical section through the same model (from Leibecker et al., 2002). Lower: Updated models of mid-crustal and upper mantle anisotropy from Gatzemeier and Moorkamp (2005). Leibecker et al. sites lie in lower left corner of Gatzemeier and Moorkamp array. Reproduced with authors' permissions.

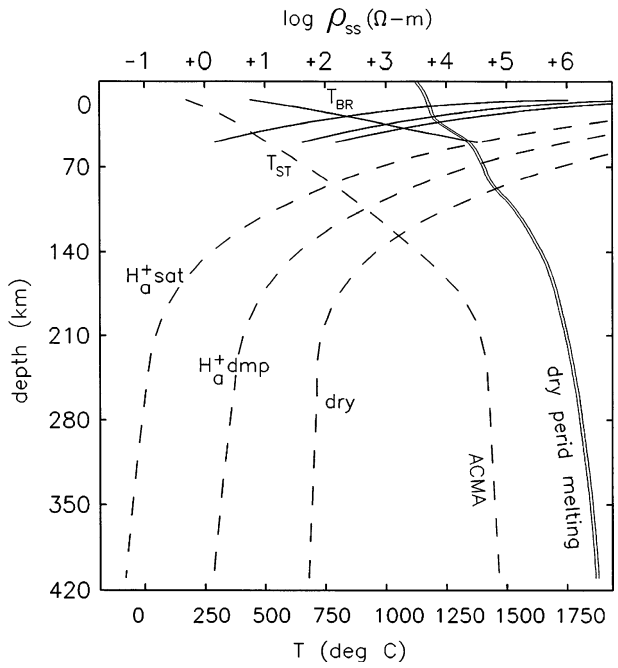

Figure 12. Predicted solid-state electrical conductivity profiles assuming high (BR, solid curves) and stable (ST, dashed curves) regime geotherms, and various states of olivine hydration. Hydration states include H_2O saturation (H^+ sat) for crystal *a*-axis, 'damp' *a*-axis olivine (dmp), and dry lherzolite (dry).

Conductivity profiles were derived for temperatures up to dry peridotite melting (Takahashi, 1986). Curves include saturated olivine along its most conductive *a*-axis (001), 3.5% saturated *a*-axis olivine (dmp), and dry olivine (lherzolite) after Duba and Constable (1993). For the 180–400 km depth range, saturated H^+/Si values are approximately 20000–70000 ppm with these coefficients, while in the 25–50 km depths of the high temperature profiles, H^+/Si is in the ~2000–4500 ppm range. The 'damp' concentrations thus would be ~30 times less than those.

Since solubility of hydrous defects in olivine in this model is pressure dependent, the enhancement over dry conductivity is more pronounced for cooler geotherms and greater depths (Figure 12). Below ~180 km, the difference in conductivity between an H-saturated *a*-axis of olivine, and dry olivine, is the equivalent of >700 K temperature change. Since the lattice conductivities in the *b* and *c* directions are ~30 times less than for the *a*-axis (Kohlstedt and Mackwell, 1998), the $H^+{}_a$-dmp curve in Figure 12 would serve as the saturated curve for the *b*–*c* axes as well. At 3.5% saturation, *b*–*c* axial conductivities differ negligibly from the dry curve. Hence, for greater degrees of saturation, one would expect a near-constant ratio of ~30 between

the *a*-axis conductivity and the *b*–*c* axial conductivities, regardless of degree of saturation. Nominally, this factor represents the maximal conductivity anisotropy which could be expected for aligned, hydrated olivine with these nominal experimental coefficients. Resistivities as low as 1 Ωm such as the more conductive direction seen by Gatzemeier and Moorkamp (2005) in principle are achievable at average mantle temperatures even for only partially saturated states.

However, to be sure, the degree of possible anisotropy and reduction in *a*-axis resistivity depicted in Figure 12 is an idealization. Solubility estimates for H^+ likely will continue to be refined, which to first order will be multipliers on the hydrous curves in the figure. The model assumes also that H^+ ion diffusivities can be used to predict conductivity accurately through the Nernst–Einstein equation (cf., Karato, 1990), and it is not clear that all hydrogen defects participate equally in conduction (Huang et al., 2005). Direct measurements of olivine conductivity due to hydrogen defects at best are very sparse. Shankland and Duba (1997) and Shankland et al. (1997) report on olivine *a*-axis conductivity measurements under controlled, albeit low, $f(H_2)$. They did observe a nearly linear dependence of conductivity on H_2 fugacity, confirming ionic conduction in the defect model, though again absolute density of H^+/Si remains uncertain. The prior uncertainties make difficult the prospect of quantifying degree of hydration of the upper mantle through electrical conductivity estimates.

The simple alignment of olivine represented in Figure 12 also is idealized when the diluting effects of other mantle minerals such as orthopyroxene, and especially finite development of crystal alignment, are considered (Simpson, 2002; Simpson and Tommasi, 2005). These effects may reduce likely natural anisotropies to well below the ~30:1 in the prior hypothetical discussion. Moreover, recent high-pressure experiments and simulations indicate that the olivine *a*-axis may not align with the shear direction below ~250 km depth (Mainprice et al., 2005), thus hypothetically limiting the electrical anisotropy too. Presuming that the ~100:1 upper mantle anisotropy in the model of Gatzemeier and Moorkamp (2005) is not affected by still unrecognized lateral heterogeneity or coupled multi-level anisotropy (Pek and Verner, 1997; Heise and Pous, 2001, 2003), mechanisms other than aligned hydrated olivine would appear to be acting, as recognized by Gatzemeier and Moorkamp. For example, the 100–150 km depth range still is within the nominal stability regime of graphite (cf. Jones et al., 2003). Melt in horizontally sheared upper mantle does not appear to contribute much to anisotropy; melt therein tends to segregate into sheets with shallow dip, and alignment of olivine may be suppressed or may form normal to the shear direction (Holtzman et al., 2003a, 2003b). Nevertheless, the E–W low-resistivity direction is compatible with seismic shear wave splitting reviewed by the authors, and is approximately parallel to the ENE–WSW direction of

plate motion for western Europe (Prawirodirjdo and Bock, 2004). The degree of coupling between upper mantle processes and the active rifting of the Rhine graben is unclear in the electrical conductivity structure.

4.3 Fossil Transpressional Regimes

Studies in the Canadian Precambrian Shield terranes have been some of the most prominent with regards to deep electrical anisotropy, especially those of the Abitibi-Grenville provinces in the East (Jones, 1992; Kellett et al., 1992; Kurtz et al., 1993; Mareschal et al., 1994, 1995; Boerner et al., 2000). There, a pervasive resistivity anisotropy in the lowermost crust or uppermost mantle exists over a transect length of > 300 km, with the more conducting direction $\sim$N55°E parallel to observed Archean tectonic patterns. Given this length and consistency, and lack of vertical magnetic field anomalies, an equivalent causative lateral eterogeneity at depth is deemed less likely. Boerner et al. interpret the conducting element to be graphite precipitated from mantle CO_2 fluxes along crustal scale fault zones, due to lack of obvious crustal sedimentary sources. In contrast, reconnaissance isotope studies described by Mareschal et al. (1994) indicate a biogenic component dominates. Ji et al. (1996) interpreted a possible modest (20–25°) obliquity between electrical and SKS-type seismic anisotropy in the region as due to a finite degree of strain having different effects on degree of crystalline alignment versus structural macro-rotations. However, determining the exact depth interval of seismic anisotropy from SKS is notoriously difficult (e.g., Savage, 1999), and the MT phase data only were interpreted, so it is not clear to this author that the two anisotropies necessarily originate from the same depth interval.

The situation may be clearer for the Great Slave Lake shear zone where seismic backscattering analysis suggested two levels of distinct S-wave anisotropy nearly paralleling similar anisotropic trends emerging from the MT data (Eaton et al., 2004). This correspondence lead the authors to suggest that parallel seismic and MT anisotropies originated from common depth intervals, although the seismic depth intervals remain poorly constrained. Graphitic films along shear zones and hydrous defect in olivine were offered as possible mechanisms for the electrical anisotropy. Nevertheless, establishing correspondence between electrical and SKS-type seismic anisotropy remains challenging; S-wave tomography may address this problem as it has better capability for resolving depths of anisotropic S velocity, but the array requirements are more stringent (e.g., Simons and vander Hilst, 2003).

Currently, the world's longest deep crustal conductivity anomaly is that of the North American Central Plains (NACP) within the Proterozoic Trans Hudson orogen (Camfield et al., 1970; Camfield and Gough, 1977; Wu et al., 1993; Jones et al., 1993, 1997, 2005). Massive amounts of conducting material

were implied by 2D modeling and inversion of several profiles, with a greatly preferred direction of conduction along strike. In the central domain of the province in Saskatchewan, sulphides remobilized into fold hinges during deformation following original sedimentary deposition are observed to be a possible strong cause of the anisotropy (Figure 13). Further South in the Black Hills region of the northwestern US, an outcropping belt of graphitic metasediments appears to be a likely cause. Recent surveying of the probable extension of the NACP northward through Baffin Island suggests graphite as the principal cause as well (Evans et al., 2005). Graphite is also suggested as a contributor to mantle lithosphere level conductors, possibly existing as deeply down a suspected fossil suture zone as the transition to diamond at >150 km depth (Jones et al., 2003). Sulphides and graphite often are closely associated genetically and so both materials could act in different parts of the orogen.

Due to the very high conductivities of these minerals, resistivity anisotropies in the 100s or 1000s are possible if sulphides or graphite are finely interbedded with intervening silicate mineralogies, either as near-original bedding or concentrated by metamorphic remobilization (e.g., Katsube et al.,

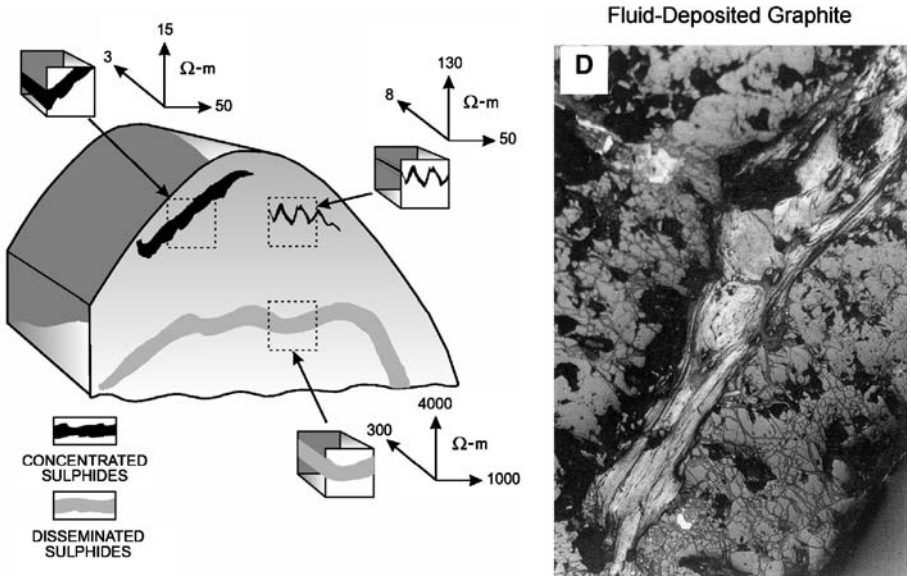

Figure 13. Left: Electrical model of carbonaceous sulphidic schist collected in central Trans Hudson Orogen MT project area, showing concentrated sulphides in folded hinges (graphic provided by Jones, further description in Jones et al., 1997). Cartesian axes show anisotropic bulk resistivities typical of different sulphide textural domains. Right: Vein of fluid deposited graphite from assimilation of organic sediments in igneous melt with subsequent slow cooling and hydrothermal circulation (graphic reproduced by permission of J. Luque; further description in Luque et al., 1998; Gervilla et al., 2002). Field of view is $\sim$3 mm across.

1996, 2003; Connell-Madore et al., 2004). Strictly speaking, neither folding nor segregation demand translational deformation along strike, even though some component of along-strike motion naturally occurs. This mechanism nevertheless contrasts with the fractal percolation or evolutionary fault element models of Figures 2 and 6 which require at least some shearing, and points out that several ways may exist to create electrical anisotropy in the Earth.

The apparent resistivities of the NACP anomaly are their most anisotropic in North Dakota (Jones et al., 2005), but perhaps this is due partly to regional current-channeling affects along strike (Camfield et al., 1970) or to obliquity between geometric strike and anisotropy strike (Pek and Verner, 1997; Heise and Pous, 2003). Indeed, phases exceeding 90° plus very steeply descending or cusplike apparent resistivities were observed by Weckmann et al. (2003) in their survey of the Namibian Damara Belt. These were modeled by an anisotropic fault zone in the upper crust (Waterberg Fault) over an anisotropic lower crust of oblique orientation. Weckmann et al. were able to fit all four elements of the impedance tensor reasonably well with this model.

The role of graphite as a cause of lower crustal conductivity has not been without controversy (Yardley and Valley, 1997; Wannamaker, 2000). In high-grade metamorphic terranes, graphite tends to form flake-like textures without the long-range interconnection needed for a sizeable MT response (Jödicke, 1988; Yardley and Valley, 1997). However, results from the German KTB drilling project and observations worldwide show that subsequent retrograde metamorphism can remobilize graphite during fluid-based leaching and redeposit it in veinlike or tabular textures which appear likelier to interconnect (ELEKTB Group, 1997; Luque et al., 1998; Eisel and Haak, 1999; Wannamaker, 2000; Eisel et al., 2001; Gervilla et al., 2002) (Figure 13). This process hypothetically may establish high deep crustal conductivity, and it may also explain the strong anisotropy often inferred to the conductors, since fluid remobilization and shear deformation along the conductive axis is likely to be greater than across the axis, bringing interconnection to the percolation threshold and beyond (Bahr, 1997; Cox et al., 2001).

Extensive broadband MT soundings have been carried out in the Fennoscandian Shield to establish electrical properties of the deep crust and upper mantle, and estimate depth to the lithosphere-asthenosphere boundary (Korja and Koivukoski, 1994; Korsman et al., 1999; Korja et al., 2002a; 2002b; Pajunpaa et al., 2002; Varentsov et al., 2002; Lahti et al., 2005). Some very strong deep crustal conductors are evident from extensive MT coverage of the region, and the BEAR working group has made considerable efforts to quantify the integrated crustal conductance as a prelude to modeling the upper mantle (Figure 14). These conductors, where possible to follow to surface, appear to be caused by major belts of graphitized biogenic material

in metasediments now deeply underthrust in Proterozoic suture zones. Strong regional conductors like these and that of the NACP are globally significant phenomena (Boerner et al., 1996; Wannamaker, 2000).

Decomposed impedance strikes with a NE–SW trend to periods of ~10,000 s lead Bahr and Simpson (2002) to suggest that the olivine in the upper mantle below southern Fennoscandia was strongly aligned despite the slow movement of the plate, thus inferring convective processes or fossil anisotropy were also contributing. However, forward modeling of the regional conductance map shows that crustal structure at least in the central-southern portion of the project area was sufficient to explain the great majority of the strikes and apparent anisotropy (Korja et al., 2002b; Lahti et al., 2005) (Figure 14). Some conductance in the upper mantle is still required to explain the longest period data, but it is unclear presently whether the variations are isotropic or anisotropic. Lahti et al. found too that MT strikes grouped into subregions over the total Fennoscandian array, also suggesting there were important lithospheric contributions.

Australia, on the other hand, is part of a fast-moving, thick coherent plate headed NNE-ward at >8 cm/year for the past 40 Myear, and at a somewhat slower rate for the previous 40 Myear (Betts et al., 2002; Prawirodirjdo and Bock, 2004). A nearly uniform orientation to S-wave fast directions, just East of North, over most of the continent for depths >200 km accompanies this motion and has been interpreted to result from shear-induced, aligned olivine (see Simons and van der Hilst, 2003, for most recent discussions). In this setting, Simpson (2001) acquired four long period soundings separated by ~200 km over Proterozoic terranes of central Australia to test for coincident electrical anisotropy. Approximately uniform axial directions of the decomposed impedances were observed at all four sites (Figure 15), with apparent anisotropy developing most strongly for periods $T > 300$ s. The inference that anisotropy lies somewhere in the upper mantle should be stronger than the case for Fennoscandia because there appeared to be negligible influence of large scale lower crustal conductors. Those appear restricted mainly to the transition (suture) to Paleozoic basement nearly 1000 km to the East (Lilley et al., 2003).

It is difficult to ensure that influence of lateral lithospheric conductivity variations is accounted for with such limited spatial sampling of sites, and so the precise depth domain and degree of the apparent anisotropy is uncertain. Also, exact depth corresponding to a strike estimate at a certain period can be clouded by the anisotropy itself due to differing penetration depths for the two modes (Jones, 2002). Nevertheless, resistor network modeling of naturally deformed peridotite with large degrees of total strain by Simpson and Tommasi (2005) suggested that sublithospheric resistivity anisotropies of 2–3 inferred for Australia (Figure 15; Simpson, 2002) were near the upper limit of what should be expected. Additional, anisotropically oriented material such

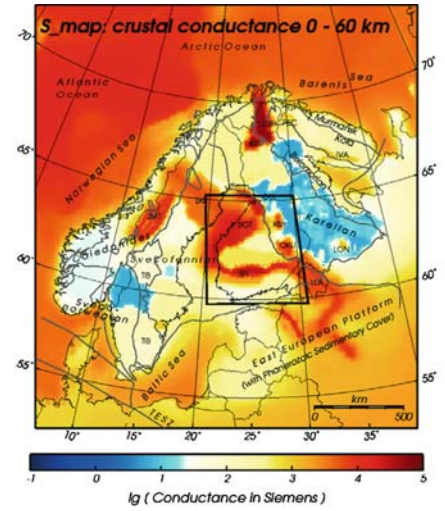
S_map: crustal conductance 0 - 60 km
Arctic Ocean
Atlantic Ocean
Barents Sea
Norwegian Sea
Karelian
Sveconorwegian
Baltic Sea
East European Platform
(with Phanerozoic Sedimentary Cover)
km
0 500
lg (Conductance in Siemens)

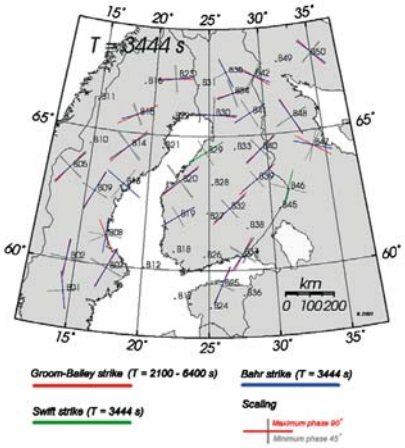
T = 3444 s
km
0 100200
Groom-Bailey strike (T = 2100 - 6400 s)
Bahr strike (T = 3444 s)
Swift strike (T = 3444 s)
Scaling

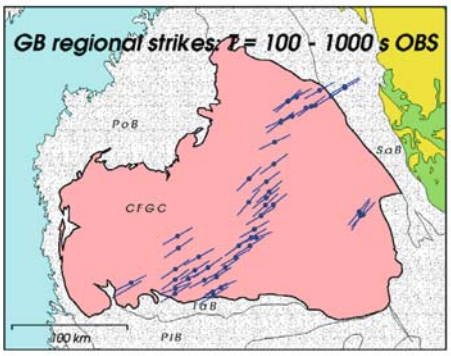
GB regional strikes: T = 100 - 1000 s OBS
PoB
SaB
CrGC
GB
100 km
PiB

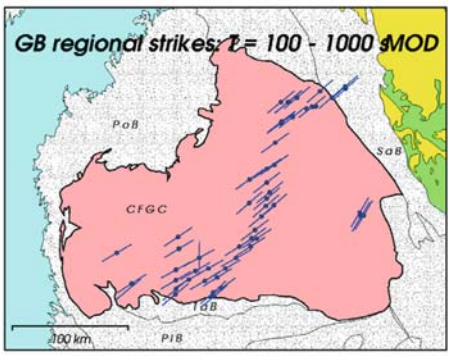
GB regional strikes: T = 100 - 1000 s MOD
PoB
SaB
CrGC
GB
100 km
PiB

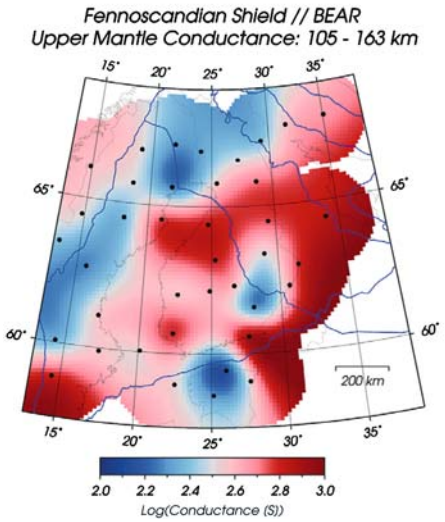
Fennoscandian Shield // BEAR
Upper Mantle Conductance: 105 - 163 km
200 km
Log(Conductance (S))

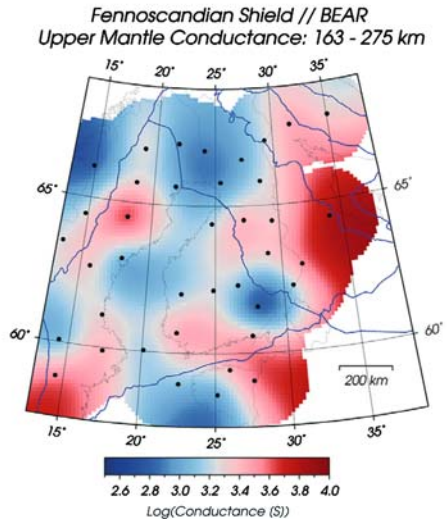
Fennoscandian Shield // BEAR
Upper Mantle Conductance: 163 - 275 km
200 km
Log(Conductance (S))

Figure 14. Upper left: Conductance map of Fennoscandian shield from 5×5 km binning of compiled crustal EM transects (mostly MT). Upper right: Impedance strike directions using both decomposed impedances and traditional Swift-type analysis generally agree well. Middle: Observed Groom–Bailey type regional strikes in south central shield (left), compared to computed Groom–Bailey strikes from the conductance model (right). Lower left and right: upper mantle conductance maps showing remaining conductivity in upper mantle needed for approximate modeling of long period data in addition to the contribution from the conductance map. All from Korja et al. (2002b) and Lahti et al. (2005), provided by T. Korja.

as graphite, or banding of olivine-rich and Fe-poor orthopyroxene, both macroscale effects, were suggested as possible supplements to the hydration for cases of high horizontal anisotropy (e.g., Gatzemeier and Moorkamp, 2005). A problem with these choices is the apparent need for vertical shearing to create horizontal anisotropy, whereas this is not obviously achieved through horizontal plate motions and shearing (Simpson and Tommasi, 2005). Experiments of very large aperature with 3D modeling are highly desirable to optimally resolve heterogeneous and anisotropic effects and their spatial extents.

The final study area considered is the Southern Appalachians fossil compressional belt of the southeastern United States. It experienced closure of two major ocean basins, one in the late Proterozoic (Grenville orogeny)

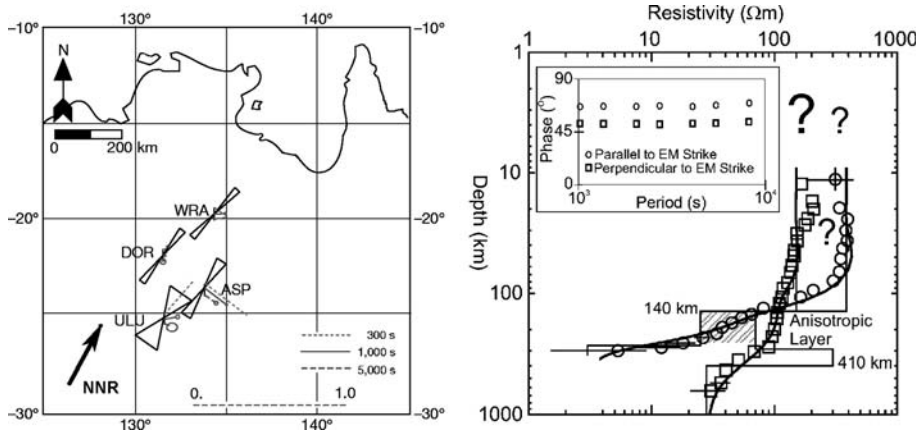

Figure 15. Left: Locations of four long period MT stations deployed in north-central Australia by Simpson (2001). Histograms at sites denote MT strikes in the period range 1000–10,000 s, interpreted by author to correspond to upper mantle depths > 150 km. Grey bars are vertical magnetic field induction arrows at various periods, indicating degree of lateral heterogeneity in the area. Solid black arrow is apparent plate motion vector in no-net-rotation (NNR) reference frame. Right: Layered resistivity-depth models for EM strike (NNE) and cross EM strike (ESE) directions at MT station DOR (Simpson, 2002), showing higher upper mantle conductivity in the former direction. Static levels in the apparent resistivity were estimated from Sq variations.

and one in the early-middle Paleozoic (Taconic), with final collision and plutonism in the Late Paleozoic (Alleghanian) (Hatcher, 1989; van Schmus et al., 1993; Rankin, 1994; Hibbard et al., 2002). Tectonic setting and problems, MT data collection, and basic response trends were discussed by Wannamaker et al. (1996), and a 2D isotropic inversion model using just the sparser long period soundings was derived by Ogawa et al. (1996). Merged wideband and long period data were inverted by Wannamaker et al. (2004) and Wannamaker (2005). Sections appear in Figure 16 incorporating (a) just the TM mode apparent resistivity and impedance phase, b) joint inversion of aforesaid TM, TE and vertical field data, and (c) vertical magnetic field and long period TE phase adhering to the TM model.

Section (a) shows two lower crustal conductive regions of modest amplitude, one near the northwest end of the line, and one near its middle. A third one may exist near the coast to the southeast but this is at the very edge of the coverage. Section (b) is a classic example of clumping of conductive material in the model when an isotropic model is forced to fit data over anisotropic structure, in particular where the TE data imply higher conductivity along the strike direction. Such clumping, seen also with the New Zealand results (Wannamaker et al., 2002), restricts current flow across strike while still permitting it along strike. It was exemplified in the synthetic results of Heise and Pous (2001) already discussed, but does not require obliquity of anisotropy strike. The preferred model section is (c), where anomalous model structure occurs in the same general locations as the TM-only model but is of higher amplitude to represent the anisotropy.

The two conductive zones near the Moho or uppermost mantle noted above are correlated with the Grenville and Taconic sutures with deep underthrusting of organic graphite-bearing metasediments down the suture zones. The collisional events exhibited strong degrees of strike slip motion, presumably promoting greater interconnection along strike. It is thus a fossil analogue to the current situation under the South Island of New Zealand,

Figure 16. Three inversion cross sections derived from MT transect across southern Appalachians compressional orogenic belt (site map and data in Wannamaker et al., 1996). Top section is TM mode only, middle section is joint TM–TE phase-vertical H-field model, and bottom is TE impedance phase and vertical magnetic field with model adherence to the TM mode section. Note clumping of lower crustal conductivity in central panel. For both (a) and (c), inversion normalized RMS misfit was ~4.5, while for b) it climbed to ~7.2. Column Apr is 1D *a priori* and starting model derived from integration of TM mode impedance across the transect. Main physiographic features include Cumberland Plateau (CP), Valley and Ridge (VR), Blue Ridge (BR), Inner Piedmont (IP), Charlotte terrane (CH), and Spring Hope terrane (SH). Geological features include New York-Alabama lineament (nyal), Pulaski fault (pl), Holston Mtn fault (hl), Grandfather Mtn window (gr), Brevard fault zone (br), Central Piedmont suture (cps), and Augusta fault zone (af).

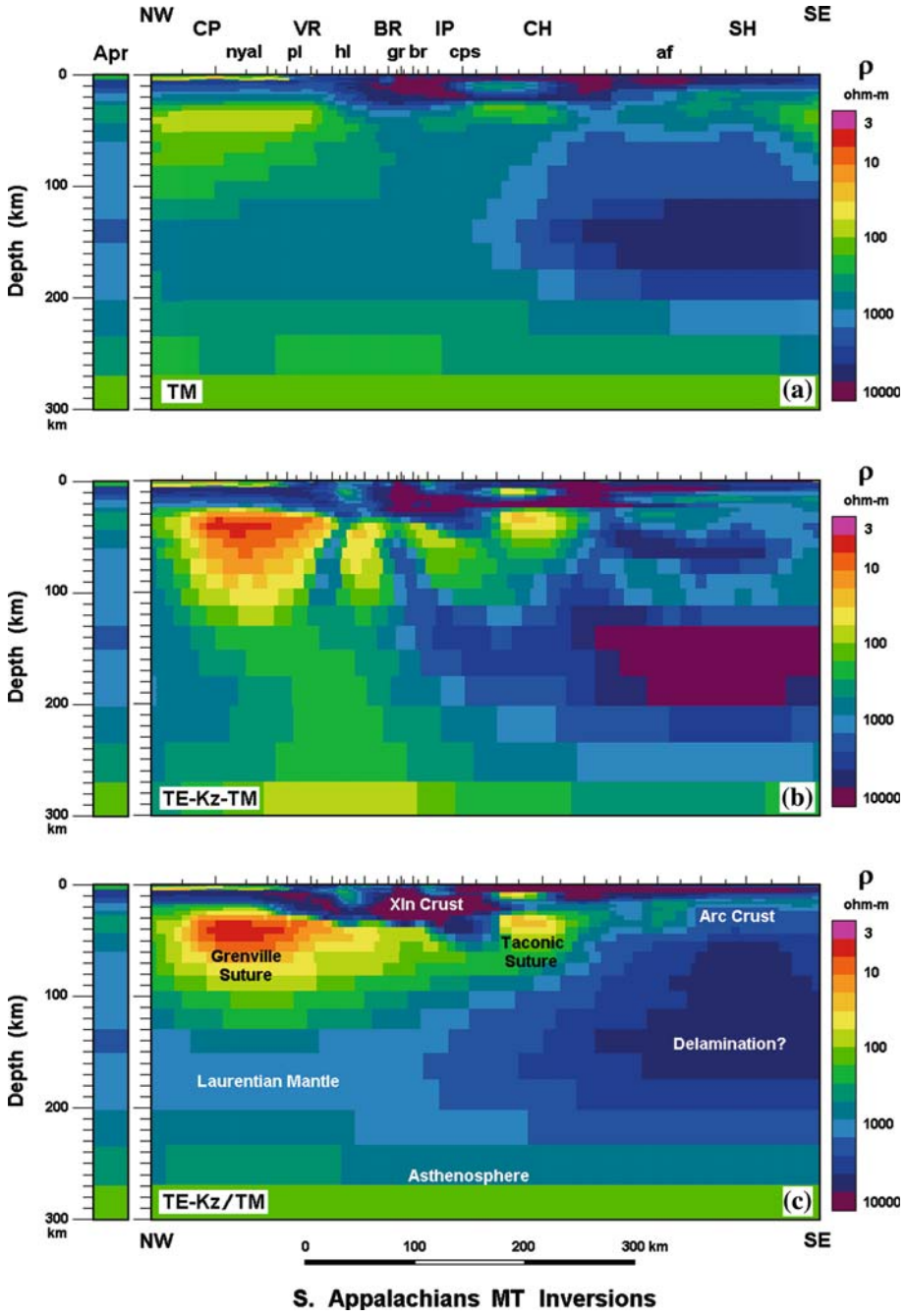

S. Appalachians MT Inversions

though at a larger scale. With graphite remobilization and deposition however, episodic fluid flow could steadily build up conductive element interconnection along strike, more so perhaps than the case with purely fluid

conductivity. Upper mantle under the Paleozoic terranes of the southeast half of the transect is much more resistive than that under the Laurentian Precambrian terranes of the northwest half (Figure 16). For the cool probable geotherm under the orogen (Goes and vander Lee, 2002), the Paleozoic mantle properties are consistent with those of pure dry olivine.

Temperatures of the Laurentian upper mantle are not expected to be higher than the Paleozoic, so the lower resistivity there suggests a greater degree of hydration is possible. A delamination or slab breakoff event at the close of the Alleghanian thought to cause an extensive suite of alkalic plutons in the southeast region (Samson et al., 1995; Bonin, 2004) may have purged the upper mantle there of volatile and low melting temperature phases, thus increasing resistivity. Null S-wave splitting occurs in the shear-wave data from the southeast (Barruol et al., 1997), which may reflect erasure of prior lithospheric fabric with the delamination. Splitting is strike-parallel (NE–SW) under the northwestern area, comparable to other compressional regimes, although the results are very sparse and the causative depth is not determined. Some contribution to S-wave splitting by the Grenville crustal suture zone structure seems possible.

5. Conclusions

Electrical conductivity anisotropy provides unique information content regarding geochemical and structural processes in the crust and upper mantle. MT data can be highly reactive to anisotropic structures and their variations with distance and depth, which in turn could represent a challenge for inversion techniques with regard to finding appropriate minima in data misfit. With the possible exception of hydrated mantle mineralogy, often it may be difficult to assume the physical scale of the oriented conducting elements causing the anisotropy due to the diminished resolving power of diffusive EM methods versus depth. Hence, an interpretation within compositional and tectonic context is necessary in order to illuminate geological causes. In the crust at least, most anisotropy identified so far appears to result from macro-scale elements such as fluidized or graphitized shear zones or deformed metasedimentary belt units, which tend to create higher conductivity along the strike of the structure. The concept of percolation threshold can be useful in that it allows small changes in regional interconnection to greatly affect bulk conductivity and thus promote anisotropy, and the theory can be physically tied to processes controlling intermittent fluid flow and deposition of conducting elements. The strong anisotropy of olivine conductivity in a hydrated solid state has potential for assessing water activity of the upper mantle, with implications for rheology and fertility to melting, but paucity of experimental work on hydrogen-induced conductivities and

uncertainty about alternate mechanisms limits quantification of hydration state at present. However, confident assessment of upper mantle anisotropy itself requires close attention to the distorting effects of lithospheric structure through appropriately comprehensive MT data modeling.

Acknowledgments

This work was supported by US National Science Foundation grants EAR02–36553 and 30027, and US Department of Energy contracts DE-FG07–00ID13891 and 04GO14297. I am very grateful to all those who contributed material for this paper and I apologize to those whose works I could not include. Very useful comments were given in reviews by Fiona Simpson and an anonymous referee. The author was saddened to hear of the passing of Hartmut Jödicke, a leading and warmly regarded researcher on lithospheric anisotropy and its mechanisms, while this paper was undergoing revision. Associate Editor John Weaver and the organizers of the 17th biennial EM induction workshop are thanked for their hard work and patience in seeing this contribution take form.

References

Adam, A.: 1996. 'Regional Magnetotelluric (MT) Anisotropy in the Pannonan Basin (Hungary)', *Acta. Geod. Geophys. Hung.* **31**, 191–216.

Baba, K.: 2005, 'Electrical Structure in Marine Tectonic Settings', *Geophys. Surveys*, this issue, 2005.

Baba, K., Chave, A.D., Evans, R. L., Hirth, G., Mackie, R. L.: 2005, 'Mantle Dynamics Beneath the East Pacific Rise at 17 S: Insights from the MELT EM Data', *J. Geophys. Res.*, in press, 2005.

Bahr, K.: 1988. 'Interpretation of the Magnetotelluric Impedance Tensor: Regional Induction and Local Telluric Distortion', *J. Geophys.* **62**, 119–127.

Bahr, K.: 1997. 'Electrical Anisotropy and Conductivity Distribution Functions of Fractal Random Networks and of the Crust: The Scale Effect of Connectivity', *Geophys J. Int.,* **130**, 649–660.

Bahr, K.: 2000. 'Percolation in the Crust Derived from Distortion of Electric Fields', *Geophys. Res. Lett.* **27**, 1049–1052.

Bahr, K. and Duba, A.: 2000, 'Is the Asthenosphere Electrically Anisotropic?', *Earth Planet. Sci. Lett.*, **178**, 2000.

Bahr, K., and Simpson, F.: 2002. 'Electrical Anisotropy Below Slow and Fast-Moving Plates: Paleoflow in the Upper Mantle?', *Science* **295**, 1270–1272.

Bahr, K., Smirnov, M., and Steveling, E., BEAR working group.: 2002. 'A Gelation Analogy of Crustal Formation Derived from Fractal Conductive Structures', *J. Geophys. Res.* **107**, 2314doi: 10.1029/2001JB000506.

Barruol, G., Silver, P. G., and Vauchez, A.: 1997. 'Seismic Anisotropy in the Eastern United States: Deep Structure of a Complex Continental Plate', *J. Geophys. Res.* **102**, 8329–8348.

Bell, D. R., Rossman, G. R., Maldener, J., Endisch, D. and Rauch, F.: 2003, 'Hydroxide in Olivine: A Quantitative Determination of the Absolute Amount and Calibration of the IR Spectrum', *J. Geophys. Res.*, **108**, doi: 10.1029/2001JB000679, 2003.

Betts, P. G., Giles, D., Lister, G. S., and Frick, L. R.: 2002. 'Evolution of the Australian Plate', *Aust. J. Earth Sci.* **49**, 661–695.

Blundell D. Freeman R . Mueller S. (eds.): 1992, *A Continent Revealed: The European Geotraverse*, University of Cambridge Press, New York 275.

Boerner, D. E., Kurtz, R. D., and Craven, J. A.: 1996. 'Electrical Conductivity and Paleo-Proterozoic Foredeeps', *J. Geophys. Res.* **101**, 13,775–13,791.

Boerner, D.E., Kurtz, R. D., and Craven, J. A.: 2000. 'A Summary of Electromagnetic Studies on the Abitibi-Grenville Transect', *Can. J. Earth Sci.* **37**, 427–437.

Bonin, B.: 2004. 'Do Coeval Mafic and Felsic Magmas in Post-collisional to Within-plate Regimes Necessarily Imply two Contrasting, Mantle and Crustal, Sources? A Review', *Lithos* **78**, 1–24.

Brasse, H., and Soyer, W.: 2001. 'A Magnetotelluric Survey in the Southern Chilean Andes', *Geophys. Res. Lett.* **28**, 3757–3760.

Camfield, P. A., and Gough, D. I.: 1977. 'A Possible Proterozoic Plate Boundary in North America', *Can. J. Earth Sci.* **14**, 1229–1238.

Camfield, P. A., Gough D., I., and Porath, H.: 1970. 'Magnetometer Array Studies in the Northwestern United States and Southwestern Canada', *Geophys. J. Roy. Astr. Soc.* **22**, 201–222.

Connell-Madore, S., Hunt, P., and Li, J.: 2004. 'Electrical Conductivity Mechanism of Graphitic Shale from the Astarte River Formation, Piling Group, Baffin Island, Nunavut', *Geol. Surv. Can. Curr. Res.* **2004-C5**, 1–9.

Cox, S. F., Braun, J., and Knackstedt, M. A.: 2001. 'Principles of Structural Control on Permeability and Fluid Flow in Hydrothermal Systems', *Rev. Econ. Geol.* **14**, 1–24.

Davydycheva, S. and Drushkin, V.: 1999, 'Staggered Grid for Maxwell's Equations in 3-D Anisotropic Media', in: M. Oristaglio and B. Spies (eds.), *Three-dimensional Electromagnetics*, Geophys. Dev. Series, 7, Soc. Explor. Geophys., Tulsa, OK, pp. 138–145, 1999.

Duba, A., and Constable, S.: 1993. 'The Electrical Conductivity of Herzolite', *J. Geophys. Res.* **98**, 11,885–11,899.

Eaton, D. W., Jones, A. G., and Ferguson, I. J.: 2004. 'Lithospheric Anisotropy Structure inferred from Collocated Teleseismic and Magnetotelluric Observations: Great Slave Lake Shear Zone, Northern Canada', *Geophys. Res. Lett.* **31**, 1961–1964.

Edwards, R. N., Nobes, D. C., and Gomez-Trevino, E.: 1984. 'Offshore Electrical Exploration of Sedimentary Basins: The Effects of Anisotropy in Horizontally Isotropic Layered Media', *Geophysics* **49**, 566–580.

Eisel, M., and Haak, V.: 1999. 'Macro-anisotropy of the Electrical Conductivity of the Crust: A Magnetotelluric Study from the German Continental Deep Drilling site (KTB)', *Geophys. J. Int.* **136**, 109–122.

Eisel, M., Haak, V., Pek, J., and Cerv, V.: 2001. 'A Magnetotelluric Profile across the German Deep Drilling Project (KTB) area: Two- and Three-dimensional Modeling Results', *J. Geophys. Res.* **106**, 16,061–16,073.

ELEKTB Group.: 1997. 'KTB and the Electrical Conductivity of the Crust', *J. Geophys. Res.* **102**, 18,289–18,306.

Evans, S., Jones, A. G., Spratt, J. and Katsube, J.: 2003, 'Central Baffin Electromagnetic Experiment (CBEX), Phase 2', Current Research, v. C-24, Geol. Surv. Can., 12 pp.

Gatzemeier, A. and Moorkamp, M.: 2005, '3-D Modeling of Electrical Anisotropy from Electromagnetic Array Data: Hypothesis Testing for Different Upper Mantle Conduction Mechanisms', *Phys. Earth Planet. Inter.*, **149**, 225–242.

Gervilla, F., Gutierrez-Narbona, R., and Fenoll Hach-ali, P.: 2002. 'The Origin of Different Types of Magmatic Mineralizations from Small-volume Melts in the Lherzolite Massifs of the Serrania de Ronda (Malaga, Spain)', *Bol. Soc. Espanola Mineral. (English trans.)* **25**, 79–96.

Goes, S. and van der Lee, S.: 2002, 'Thermal Structure of the North American Uppermost Mantle Inferred from Seismic Tomography', *J. Geophys. Res.*, **107**, 10.1029/2000JB000049.

Gueguen, Y., David, C., and Gavrilenko, P.: 1991. 'Percolation Networks and Fluid Transport in the Crust', *Geophys. Res. Lett.* **18**, 931–934.

Hammond, W. C. and Thatcher, W.: 2004, 'Contemporary Tectonic Deformation of the Basin and Range Province, Western United States: 10 Years of Observation with the Global Positioning System', *J. Geophys. Res.*, **109**, doi:10.1029/2003JB002746.

Hatcher, R.D. Jr.: 1989, 'Tectonic Synthesis of the U.S. Appalachians', in R. D. Hatcher Jr., W. A. Thomas, and G. W. Viele (eds.), *The Appalachian-Ouachita Orogen in the United States: The Geology of North America*, F-2, Geol. Soc. Amer., Boulder, CO, pp. 511–535.

Heise, V., and Pous, J.: 2001. 'Effects of Anisotropy on the Two-dimensional Inversion Procedure', *Geophys. J. Int.* **147**, 610–621.

Heise, V., and Pous, J.: 2003. 'Anomalous Phases Exceeding 90° in Magnetotellurics: Anisotropic Model Studies and a Field Example', *Geophys. J. Int.* **155**, 308–318.

Hibbard, J. P., Stoddard, E. F., Secor, Jr. D. T. and Dennis, A. J.: 2002, 'The Carolina Zone: Overview of Neoproterozoic to early Paleozoic Peri-Gondwanan Terranes along the East Flank of the Southern Appalachians', *Earth Sci. Rev.*, **57**, 299-339.

Holtzman, B. K., Groebner, N. J., Zimmerman, M. E., Ginsberg, S. B. and Kohlstedt, D. L.: 2003a, 'Stress-driven Melt Segregation in Partially Molten Rocks', *Geochem. Geophys. Geosyst.*, **4**(5), 8607, doi: 10.1029/2001GC000258.

Holtzman, B. K., Kohlstedt, D. L. and Zimmerman, M. E.: 2003b, 'Melt Segregation and Strain Partitioning: Implications for Seismic Anisotropy and Mantle Flow', *Science*, **301**, 1227–1230.

Huang, X., Xu, Y., and Karato, S.-I.: 2005. 'Water Content in the Transition Zone from Electrical Conductivity of Wadsleyite and Ringwoodite', *Nature* **434**, 746–749.

Ji, S., Rondenay, S., Mareschal, M., and Senechal, G.: 1996. 'Obliquity between Seismic and Electrical Anisotropies as a Potential Indicator of Movement Sense for Ductile Shear Zones in the Upper Mantle', *Geology* **24** (11), 1033–1036.

Jödicke, H.: 1988. 'Water and Graphite in the Earth's Crust – An Approach to Interpretation of Conductivity Models', *Surv. Geophys.* **13**, 381–407.

Jones, A. G.: 1992. 'Electrical Properties of the Continental Lower Crust', in D. M. Fountain, R. J. Arculus, and R. W. Kay (eds.), *Continental Lower Crust*, Elsevier, New York, pp. 81–143.

Jones, A. G.: 2002, 'Looking into the Earth with Polarized Spectacles', paper presented at 16th Biennial EM Induction Workshop, Santa Fe, U.S.A., June 16–22.

Jones, A. G., Craven, J. A., McNiece, G. W., Ferguson, I. J., Boyce, T., Farquarson, C., and Ellis, R.: 1993. 'North American Central Plains Conductivity Anomaly within the Trans-Hudson Orogen in Northern Saskatchewan, Canada', *Geology* **21**, 1027–1030.

Jones, A. G., Katsube, T. J., and Schwann, P.: 1997. 'The Longest Conductivity Anomaly in the World Explained: Sulphides in Fold Hinges Causing very High Electrical Anisotropy', *J. Geomagn. Geoelectr.* **49**, 1619–1629.

Jones, A. G., Lezaeta, P., Ferguson, I. J., Chave, A. D., Evans, R. L., Garcia, X., and Spratt, J.: 2003. 'J. Spratt, The Electrical Structure of the Slave Craton', *Lithos* **71**, 505–527.

Jones, A. G., Ledo, J. and Ferguson, I. J.: 2005, 'Electromagnetic Images of the Trans Hudson Orogen: The North American Central Plains Anomaly Revealed', *Can. J. Earth Sci.*, in press, 2005.

Karato, S.: 1990. 'The Role of Hydrogen in the Electrical Conductivity of the Upper Mantle', *Nature* **347**, 272–273.

Katsube, T. J., Best, M. E. and Jones, A. G.: 1996, 'Electrical Anisotropy of Mineralized and Non-mineralized rocks', Ext. Abstr., 66th Ann. Mtg. Soc. Explor. Geophys., Denver, v. II, 1279–1281.

Katsube, T. J., Keating, P. B., Connell, S, Best, M. E., and Mwneifumbo, C. J.: 2003. 'Electrical Anisotropic Characteristics of Mineralized and Unmineralized Rocks in the Bathurst Mining Camp: Implications for Airborne Conductivity Interpretation', *Econ. Geol. Mono*. **11**, 861–877.

Kellett, R. L., Mareschal, M., and Kurtz, R. D.: 1992. 'A Model of Lower Crustal Electrical Anisotropy for the Pontiac Subprovince of the Canadian Shield', *Geophys. J. Int*. **111**, 141–150.

Kohlstedt, D.., and Mackwell, S.: 1998. 'Diffusion of Hydrogen and Intrinsic Point Defects in Olivine Z', *Phys. Chem*. **207**, 147–162.

Korja, T. and Koivukoski K.: 1994, 'Crustal Conductors along the SVEKA Profile in the Fennoscandian (Baltic) Shield, Finland', *Geophys. J. Int*., **116**, 173–197.

Korja, T., Engels, M., Lahti, I., Kobzova, V., and Ladanivskyy, B.: 2002a. 'BEAR Working Group, Crustal Conductivity in Fennoscandian Shield', *Earth Planets Space* **54**, 535–558.

Korja, T., Engels, M., Lahti, I., Kobzova, V., Ladanivskyy, B. and BEAR Working Group.: 2002b, 'Is Lithosphere Anisotropic in the Central Fennoscandian Shield?, paper presented at 16th biennial EM induction workshop, Santa Fe, U.S.A., June 16–22.

Korsman, K., Korja, T., Pajunen, M., and Virransalo, P.: 1999. 'GGT/SVEKA Working Group, The GGT/SVEKA Transect: Structure and Evolution of the Continental Crust in the Paleoproterozoic Svecofennian Orogen in Finland', *Int. Geol. Rev*. **41**, 287–333.

Kovacikova, S., and Pek, J.: 2002a. 'Generalized Riccati Equations for 1-D Magnetotelluric Impedances over Anisotropic Conductors. Part I: Plane Wave Field Model', *Earth Planets Space* **54**, 473–482.

Kovacikova, S., and Pek, J.: 2002b. 'Generalized Riccati Equations for 1-D Magnetotelluric Impedances over Anisotropic Conductors. Part II: Non-uniform Source Field Model', *Earth Planets Space* **54**, 483–491.

Kurtz, R. D., Craven, J. A., Niblett, E. R., and Stevens, R. A.: 1993. 'The Conductivity of the Crust and Mantle Beneath the Kapuskasing Uplift: Electrical Anisotropy in the Upper Mantle', *Geophys. J. Int*. **113**, 483–498.

Lachenbruch, A. H. and Sass, J. H.: 1978, 'Models of an Extending Lithosphere and Heat Flow in the Basin and Range Province', Geol. Soc. Amer. Mem. 152, Boulder, CO, pp. 209–250.

Lahti, I., Korja, T., Kaikkonen, P. and BEAR Working Group.: 2005, 'Decomposition Analysis of the BEAR Magnetotelluric Data: Implications for the Upper Mantle Conductivity in the Fennoscandian Shield', *Geophys. J. Int*., in press, 2005.

Leibecker, J., Gatzemeier, A., Honig, M., Kuras, O., and Soyer, W.: 2002. 'Evidence of Electrical Anisotropic Structures in the Lower Crust and Upper Mantle Beneath the Rhenish Shield', *Earth Planet Sci. Lett*. **202**, 289–302.

Li, Y., Pek, J. and Brasse, H.: 2004, 'Magnetotelluric Inversion for 2-D Anisotropic Conductivity', paper presented at the 17th Biennial Induction Workshop, Hyderabad, August 18–23.

Lilley, F. E. M., Wang, L. J., Chaumalaun, F. H. and Ferguson, I. J.: 2003, 'Carpentaria Electrical Conductivity Anomaly, Queensland, as a Major Structure in the Australian

Plate', in R. R. Hillis and R. D. Muller (eds.), *Evolution and Dynamics of the Australian Plate*, Geol. Soc. Austral. Spec. Publ. vol. 22, pp. 141–156.

Lizarralde, D., Chave, A., Hirth, G., and Schultz, A.: 1995. 'Northeastern Pacific Mantle Conductivity Profile from Long-Period Magnetotelluric Sounding using Hawaii-to-California Submarine Cable Data', *J. Geophys. Res.* **100**, 17, 837–17, 854.

Luque, F.J., Pasteris, J.D., Wopenka, B., Rodas, M., and Barrenechea, J.F., 1998, Natural fluid-deposited graphite: mineralogical characteristics and mechanisms of formation, Amer. J Sci., **298**, 471–498.

Mainprice, D., Tommasi, A., Couvy, H., Cordier, P., and Frost, D.J.: 2005. 'Pressure Sensitivity of Olivine Slip Systems and Seismic Anisotropy or the earth's Upper Mantle', *Nature* **433**, 731–733.

Mareschal, M., Kurtz, R. D., and Bailey, R. C.: 1994. 'A Review of Electromagnetic Investigations in the Kapuskasing Uplift and Surrounding Regions: Electrical Properties of Key Rocks', *Can. J. Earth Sci.* **31**, 1042–1051.

Mareschal, M., Kellett, R. L., Kurtz, R. D., Ludden, J. N., Ji, S., and Bailey, R. C.: 1995. 'Archaean Cratonic Roots, Mantle Shear Zones, and Deep Electrical Anisotropy', *Nature* **375**, 134–137.

Ogawa, Y., Jones, A. G., Unsworth, M. J., Booker, J. R., Lu, X., Craven, J., Roberts, B., Parmalee, J., and Farquharson, C.: 1996. 'Deep Electrical Conductivity Structures of the Appalachian Orogen in the Southeastern US', *Geophys. Res. Lett.* **23**, 1597–1600.

Pajunpaa, K., Lahti, I., Olafsdottir, B., and Korja, T.: 2002. 'BEAR Working Group, Crustal Conductivity Anomalies in Central Sweden and Southwestern Finland, Geophys', *J. Int.* **150**, 695–705.

Pek, J.: 2002. 'Spectral Magnetotelluric Impedances for an Anisotropic Layered Conductor', *Acta Geophysica Polonica* **50**, 619–643.

Pek, J., and Santos, F. A. M.: 2002. 'Magnetotelluric Impedances and Parametric Sensitivities for 1-D Anisotropic Layered Media', *Comput. Geosci.* **28**, 939–950.

Pek, J. and Toh, H.: 2001, 'Numerical Modeling of MT Fields in 2-D Anisotropic Structures with Topography and Bathymetry Considered', in Hordt A., J. Stoll, eds., *Electromagnetische Ienforschung*, Protokoll uber das 18, Kolloquium, Altenberg, Germany, DGG, 190–199.

Pek, J., and Verner, T.: 1997. 'Finite-Difference Modeling of Magnetotelluric Fields in Two-dimensional Anisotropic Media', *Geophys. J. Int.* **128**, 505–521.

Prawirodirjdo, L. and Bock, Y.: 2004, 'Instantaneous Global Plate Motions from 12 Years of Continuous GPS Observations', *J. Geophys. Res.*, **109**, doi:10.1029.2003JB002944.

Rankin, D. W.: 1994, 'Continental Margin of the Eastern United States: Past and Present', in R. C. Speed (ed.), *Phanerozoic Evolution of North American Continent–Ocean Transitions*, GSA DNAG Series, pp. 129–218.

Reddy, I. K., and Rankin, D.: 1975. 'Magnetotelluric Response of Laterally Inhomogeneous and Anisotropic Structure', *Geophysics* **40**, 1035–1045.

Rodi, W. L., and Mackie, R. L.: 2001. 'Nonlinear Conjugate Gradients Algorithm for 2-D Magnetotelluric Inversion', *Geophysics* **66**, 174–187.

Samson, S. D., Coler, D. G., and Speer, J. A.: 1995. 'Geochemical and Nd–Sr–Pb Isotopic Composition of Alleghanian Granites of the Southern Appalachians: Origin, Tectonic Setting and Source Characterization', *Earth Planet Sci. Lett.* **134**, 359–376.

Savage, M. K.: 1999. 'Seismic Anisotropy and Mantle Deformation: What have we Learned from Shear Wave Splitting?', *Rev. Geophys.* **37**, 65–106.

Sawyer, E. W.: 2001. 'Melt Segregation in the Continental Crust: Distribution and Movement of Melt in Anatectic Rocks', *J. Metamorphic Geol.* **19**, 291–309.

Shankland, T. J. and Duba, A. G.: 1997. 'Correlation of Olivine Electrical Conductivity Change with Water Activity', EOS Trans. AGU, supplement, abstract T52D-10.

Shankland, T. J., Duba, A. G. and Mathez, E. H.:1997, 'The Role of Carbon and Temperature in Determining Electrical Conductivity of Basins, Crust and Mantle', U.S. Dept. of Energy, Basic Energy Sciences, Geoscience Research Program Annual Summary, contract W-7405-ENG-36.

Sibson, R. H.: 2000. 'A Brittle Failure Mode Plot Defining Conditions for High-flux Fluid Flow', *Econ. Geol.* **95**, 41–48.

Simons, F., and van der Hilst, R. D.: 2003. 'Seismic and Mechanical Anisotropy and the Past and Present Deformation of the Australian Lithosphere', *Earth Planet Sci. Lett.* **211**, 271–286.

Simpson, F.: 2001. 'Resistance to Mantle Flow Inferred from the Electromagnetic Strike of the Australian Upper Mantle', *Nature* **412**, 632–635.

Simpson, F.: 2002. 'Intensity and Direction of Lattice-preferred Orientation of Olivine: Are Electrical and Seismic Anisotropies of the Australian Mantle Reconcilable?', *Earth Planet. Sci. Lett.* **203**, 535–547.

Simpson, F. and Tommasi, A.: 2005, 'Hydrogen Diffusivity and Electrical Anisotropy of a Peridotite Mantle, *Geophys. J. Int.*, doi: 10.1111/j.1365–246X.2005.02563.x, 11 pp.

Sodergren, T. L.: 2002, 'Deep Fluid State and Thermal Regime of the Central Great Basin, Nevada, Inferred from Electrical Resistivity', M.S. thesis, Univ. of Utah, 44 pp.

Takahashi, E.: 1986. 'Melting of a Dry Peridotite KLB-1 up to 14 Gpa: Implications on the Origin of Peridotitic Upper Mantle', *J. Geophys. Res.* **91**, 9367–9382.

Tarantola, A.: 1987, *Inverse Problem Theory*, Elsevier, New York 613.

Thompson, A. B.: 1992. 'Water in the Earth's Upper Mantle', *Nature* **358**, 295–302.

Torres-Verdin, C., and Bostick, F. X. Jr.: 1992. 'Principles of Spatial Surface Electric Field Filtering in Magnetotellurics: Electro-magnetic Array Profiling (EMAP)', *Geophysics* **57**, 603–622.

Tullis, J., Yund, R. A., and Farver, J: 1996. 'Deformation-enhanced Fluid Distribution in Feldspar Aggregates and Implications for Ductile Shear Zones', *Geology* **24**, 63–66.

Van Schmus, W. R., Bickford, M. E., Anderson, J. L., Bender, E. E., Anderson, R. R., Bauer, P. W., Robertson, J. M., Bowring, S. A., Condie, K. C., Denison, R. E., Gilbert, M. C., Grambling, J. A., Mawer, C. K., Shearer, C. K., Hinze, W. J., Karstrom, K. E., Kisvarsanyi, E. B., Lidiak, E. G., Reed, J. C., Jr., Sims, P. K., Tweto, O., Silver, L. T., Treves, S. B., Williams, M. L. and Wooden, J. L.: 1993, 'Transcontinental Proterozoic Provinces', in: J. C. Reed, Jr, M. E. Bickford, R. S. Houston, P. K. Link, D. W. Rankin, P. K. Sims, W. R. Van Schmus, (eds.), *Precambrian: Coterminous U.S., The Geology of North America*, C-2, Geol. Soc. Amer., Boulder CO, pp. 171–334.

Varentsov, I. M., Engels, M., Korja, T., and Smirnov, M. Y.: 2002. 'The BEAR Working Group, A Generalized Geoelectric Model of Fennoscsandia: A Challenging Database for Long-period 3D Modeling Studies within the Baltic Electromagnetic Array Research (BEAR) Project, Izvestiya', *Phys. Solid Earth* **38** (10), 855–896.

Wang, T., and Fang, S.: 2001. '3-D Electromagnetic Anisotropy Modeling Using Finite Differences', *Geophysics* **66**, 1386–1398.

Wannamaker, P. E.: 2000, 'Comment on ''The petrologic case for a dry lower crust'', by B. D. Yardley and J. W. Valley', *J. Geophys. Res.*, **105**, 6057–6064.

Wannamaker, P. E.: 2005, 'The Electromagnetic View of Continental Dynamics: U.S. Experience and the Potential of Earthscope', Decadal vision session, Earthscope National Meeting (www.earthscope.org), Tamayo Lodge, NM, March 28–31.

Wannamaker, P. E., and Doerner, W. M.: 2002. 'Crustal Structure of the Ruby Mountains and Southern Carlin Trend Region, Northeastern Nevada, from Magnetotelluric Data', *Ore Geol. Rev*. **21**, 185–210.

Wannamaker, P. E., Chave, A. D., Booker, J. R., Jones, A.G., Filloux, J. H., Ogawa, Y., Unsworth, M., Tarits, P., and Evans, R.: 1996. 'Magnetotelluric Experiment Probes Deep Physical State of Southeastern U.S., EOS article', *Trans. AGU* **329**, 332–333.

Wannamaker, P. E., Doerner, W. M., Stodt, J. A., and Johnston, J. M.: 1997. 'Subdued State of Tectonism of the Great Basin Interior Relative to its Eastern Margin based on Deep Resistivity Structure', *Earth Planet. Sci. Lett*. **150**, 41–53.

Wannamaker, P. E., Bartley, J. M., Sheehan, A. F., Jones, C. H., Lowry, A. R., Dumitru, T. A., Ehlers, T. A., Holbrook, W. S., Farmer, G. L., Unsworth, M. J., Hall, D. B., Chapman, D. S., Okaya, D. A., John, B. E. and Wolfe, J. A.: 2001, 'Great Basin–Colorado Plateau Transition in Central Utah: An Interface between Active Extension and Stable Interior', in M. C. Erskine J. E. Faulds J. M. Bartley and P. Rowley (eds.), *The Geological Transition: Colorado Plateau to Basin and Range*, Proc. J. Hoover Mackin Symposium, UGA/AAPG Guideb. 30/GB78, Cedar City, Utah, September 20–23, pp. 1–38.

Wannamaker, P. E., Jiracek, G. R., Stodt, J. A., Caldwell, T. G., Porter, A. D., Gonzalez, V. M. and McKnight, J. D.: 2002, 'Fluid Generation and Movement beneath an Active Compressional Orogen, the New Zealand Southern Alps, Inferred from Magnetotelluric (MT) Data, *J. Geophys. Res*., **107**(B6), ETG 6 1–22.

Wannamaker, P. E., Unsworth, M. J., Jones, A. G., Chave, A. D., Ogawa, Y. and Booker, J. R.: 2004, 'Lithospheric Architecture and Physical State below the Southern Appalachians Compressional Orogen from Electrical Conductivity structure', paper presented at 17th International Basement Tectonics Conference '4-D framework of Continental Crust', Oak Ridge, June 27-July 1.

Watson, E. B., and Brenan, J. M.: 1988. 'Fluids in the Lithosphere, 1. Experimentally-determined Wetting Characteristics of CO_2–H_2O Fluids and their Implications for Fluid Transport, Host-rock Physical Properties, and Fluid Inclusion Formation', *Earth Planet. Sci. Lett*. **85**, 497–515.

Weckmann, U., Ritter, O., and Haak, V.: 2003. 'A Magnetotelluric Study of the Damara Belt in Namibia 2. MT Phases over 90° Reveal the Internal Structure of the Waterberg Fault/Omaruru Lineament', *Phys. Earth Planet. Inter*. **138**, 91–112.

Weidelt, P.: 1999, '3-D Conductivity Models: Implications of Electrical Anisotropy', in M. Oristaglio and B. Spies (eds.), *Three-dimensional Electromagnetics*, Geophys. Dev. Series, 7, Soc. Explor. Geophys., Tulsa, OK, pp. 119–137.

Weiss, C. J., and Newman, G. A.: 2002. 'Electromagnetic Induction in a Fully 3-D Anisotropic Earth', *Geophysics* **67**, 1104–1114.

Wu, N., Booker, J. R., and Smith, J. T.: 1993. 'Rapid Two-dimensional Inversion of COPROD2 Data', *J. Geomagn. Geoelectr*. **45**, 1073–1087.

Yardley, B. W. D., and Valley, J. W.: 1997. 'The Petrologic Case for a Dry Lower Crust', *J. Geophys. Res*. **102**, 12,173–12,185.

Zhao, Y.-H., Ginsberg, S. B., and Kohlstedt, D. L.: 2004. 'Solubility of Hydrogen in Olivine: Dependence on Temperature and Iron Content', *Contrib. Min. Petr*. **147**, 155–161.

Zoback, M. L., McKee, E. H., Blakely, R. J., and Thompson, G. A.: 1994. 'The Northern Nevada Rift: Regional Tectono-magmatic Relations and Middle Miocene Stress Direction', *Geol. Soc. Amer. Bull*. **106**, 371–382.